THE ASTROPHYSICAL JOURNAL, 292:104–121, 1985 May 1

THE CORES OF ELLIPTICAL GALAXIES[1]

TOD R. LAUER
Lick Observatory, Board of Studies in Astronomy and Astrophysics, University of California, Santa Cruz
Received 1984 September 10; accepted 1984 November 6

ABSTRACT

Core radii and central surface brightnesses are measured from seeing-deconvolved high-resolution CCD surface photometry profiles for 42 nearby elliptical galaxies presented in Paper I. Analysis of the apparent core radii and seeing profiles indicates that 14 galaxies have resolvable cores between 1".5 and 5".0. None of the resolved cores can be described by isothermal King model cores. Half of the resolved galaxies match the core profile of M87 over an extended radial range, indicating the possible existence of massive nuclear black holes or radially anisotropic velocity fields in these objects. The remaining half show even larger deviations from isothermality. Analysis of the core parameters finds that the central luminosity density, ρ_c, acts as a second parameter, along with luminosity L, in determining core structure. Central mass-to-light ratios are calculated from the core parameters; parameterization of M/L by L and ρ_c shows M/L to depend on central luminosity density only, since $M/L \propto \rho_c^{-0.17}$. Parallel results are found for average luminosity densities and mass-to-light ratios derived from the de Vaucouleurs effective radius parameters. The ratio of core radius to effective radius shows large scatter, however, and no dependence on total luminosity. The present results support the formation of elliptical galaxies from photogalactic gas clouds rather than as products of a dissipationless merger hierarchy or repeated cannibalization of less massive stellar systems. Larson's suggestion that the cores represent the final period of star formation in the cloud most easily explains the observed independence of the cores from global properties of the galaxies. The dependence of M/L on ρ_c is then explained as a possible dependence of the initial mass function (IMF) slope or lower–main-sequence cutoff on local mass density.

Subject headings: galaxies: photometry — galaxies: structure

I. INTRODUCTION

The cores of elliptical galaxies represent the high end of the stellar density distributions, and consequently the bottom of the potential wells, of these galaxies; thus the cores are an important structural component of elliptical galaxies. Knowledge of the core properties provides useful information on the structure, dynamics, and formation of elliptical galaxies. (See Binney 1982 for a review.) The size and density of the core may reflect the conditions that prevailed at galaxy formation (Larson 1974*a*), or the dynamical effects of galaxy mergers or other processes which occurred much later (Farouki, Shapiro, and Duncan 1983). The structure and environment of the central potentials may also provide useful information on the formation of active galactic nuclei. Young *et al.* (1978), for example, find that the core luminosity profile of M87 may reflect the response of the stellar system to a massive nuclear black hole. Other investigators (see Binney and Mamon 1982) have shown that the core structure may also reflect possible anisotropies in the central velocity field. Core radii and central surface brightnesses are also required to calculate central mass-to-light ratios (King and Minkowski 1972).

Unfortunately, accurate measurements of core structure are difficult to obtain. King's (1978) surface photometry profiles of elliptical galaxies show that the apparent core radii are only a few times the seeing radii in size; Schweizer (1979) has shown that without any *a priori* knowledge of the central structure of the galaxies it is difficult to conclude that King's apparent cores are due to anything other than the effects of seeing on intrinsically unresolvable cores. To investigate this problem, CCD images with high spatial resolution and high signal-to-noise ratio were obtained of a sample of 42 elliptical and S0 galaxies. Surface photometry profiles measured from these images form a new set of observations for investigating the cores of elliptical galaxies. A crucial part of this program was the accurate measurement of seeing and subsequent seeing deconvolution of the photometry. The details of the observations, their reductions, and the resulting surface photometry profiles have been presented separately (Lauer 1985*a*, hereafter Paper I). This paper considers the problem of core resolution and identifies a subset of the observed galaxies which appear to have resolvable cores under the prevailing seeing conditions. Core radii and central surface brightnesses are used to investigate the relationship of the core structure to the global properties of the galaxies. A brief discussion is then presented on implications for current theories on the formation of elliptical galaxies.

II. OBSERVATIONAL MATERIAL

To provide background for the present analysis, a summary of the observational program is presented here; the reader is referred to Paper I for a complete discussion. Briefly, direct images of the program galaxies were obtained with CCD cameras mounted at the Cassegrain focus of the Lick Observatory Nickel 1 m reflector. The observations were obtained through a 6000–7000 Å filter and were reduced to the R band by comparison with published aperture photometry. The exposure times were selected to guarantee a minimum signal-to-noise ratio of 100 in the cores. Angular resolution was limited by atmospheric seeing which had a medium FWHM of 1".69 for the sample. The seeing point-spread function (PSF) was measured from stars present in the images and was fitted by a multicomponent model which describes the PSF as a Gaussian core with exponential wings. The surface photometry profiles

[1] Lick Observatory Bulletin, No. 1000.

were extracted by fitting the galaxy images with concentric ellipses, which are found to be an excellent approximation to the true isophote shapes. The fitting procedure was optimized for high angular resolution and causes no degradation of the sharp cores of the galaxies. The profiles specify the structure of the galaxies in terms of semimajor axis surface brightness, isophote ellipticity, and position-angle profiles.

Efforts were then made to correct the surface photometry for seeing in a model-independent way. This was done by Fourier deconvolution of the seeing PSF from a smooth image reconstructed from the photometry. The reconstructed image is faithful to the structure of the original image, but has greatly reduced noise, which markedly improves the success of the deconvolution. The basic theory of deconvolution is summarized below. An astronomical image I represents the true projection of some object O onto the sky, convolved with the PSF, P, with added noise N. Therefore, I can be represented as

$$I = O * P + N . \quad (1)$$

In the Fourier domain, convolution reduces to multiplication, so

$$i = op + n . \quad (2)$$

Fourier deconvolution attempts to recover an estimate of the object, O', by dividing the image by the PSF transform and applying a Wiener (1949) filter ϕ to eliminate the noise which dominates at high spatial frequencies. The form of the filter is optimized to have minimal effect on the low spatial frequencies, where image structure dominates. In the Fourier domain, then,

$$o' = i\phi/p \quad (3a)$$

$$= o\phi + n\phi/p \quad (3b)$$

$$\approx o\phi . \quad (3c)$$

In practice, the success of the deconvolution procedure depends on the strength of noise in the image and the intrinsic sharpness of the galaxy's core. At some point, the Wiener filter is forced to cut out the high spatial frequencies in the image and therefore implicitly defines the resolution of the deconvolved image. For galaxies with well-resolved cores (see the discussion below), which have little structure on the spatial scales dominated by noise, the deconvolution procedure produces fairly modest corrections to the photometry. In the case of NGC 3379, for example, the deconvolution procedure is able to recover the luminosity distribution observed by Nieto (1983) under sub-arcsecond seeing conditions (see Paper I). For more poorly resolved galaxies, the amount of deconvolution possible is limited and even the deconvolved photometry must still be considered to have unresolved cores. Tests on simulated images shows that the dividing line between the two cases occurs when the size of the intrinsic core radius is roughly twice the seeing radius.

The effects of the deconvolution procedure can be viewed as replacing the seeing PSF in the image with a sharper PSF due to the Wiener filter. To provide some measure of the deconvolution carried out for each galaxy, values of the FWHM of the seeing PSF, Δ, and the spatial domain representation of the Wiener filter, Δ', are given in Table 1. Caution is advised in comparing the two numbers, however. The seeing PSF, which has broad wings, causes more broadening of the core than does a Gaussian of the same width, while the filter, which has little effect on the lower spatial frequencies, causes less broadening. In short, the effects of a PSF cannot be characterized simply by its width. In practice, it appears that for the particular form of the Wiener filter used, the width of the seeing PSF which would produce the same blurring as the Wiener filter is about 20% smaller than Δ'. In terms of the seeing conditions of the actual observations, this means that the final deconvolved profiles presented in Paper I have slightly sub-arcsecond resolution.

III. RESOLUTION OF THE CORES

a) Measurement of the Core Radii

The observed and deconvolved core radii, r_c and r_c', of the surface brightness profiles presented in Paper I are given in Table 1. The core radii are defined to be the HWHM of the profiles and are measured directly from them. (The radii, therefore, refer to the major axes of the galaxies.) This present definition of core radii seeks only to provide a useful scale for describing the central behavior of the luminosity profiles in a model-independent way. The random errors in these measurements are insignificant, given the quality of the surface photometry and the much larger systematic effects due to seeing (which will be discussed shortly).

Since the usefulness of the core radii depends critically on the extent to which they reflect intrinsic core structure rather than seeing effects, two criteria are introduced below to quantify the degree of core resolution of galaxies in the sample. Three resolution classes are then introduced to sort out well-resolved, marginally unresolved, and completely unresolved galaxies identified by these criteria. The major criterion for resolution is the size of the apparent cores; well-resolved galaxies must have significantly larger cores than can be produced by seeing effects on an intrinsically coreless galaxy model fitted to their envelopes. The second criterion examines the amount of core sharpening produced by the deconvolution process; the size of the deconvolved cores of well-resolved galaxies should not be strongly dependent on the limiting resolution of the deconvolution. It is clear, however, that no ultimate statement on central luminosity density can be made for even the best resolved galaxies. Small nuclear star clusters embedded in otherwise well-resolved cores may be very difficult to detect (Schweizer 1979; Djorgovski 1983). Further, the effects of seeing on very shallow power-law brightness profiles can creat extended and apparently well-resolved cores, despite the intrinsic central singularities (Bailey and Sparks 1983).

b) Comparison of the Core Radii to Seeing

The measure of core resolution that will be given the most weight is based on a comparison of the apparent core radius, r_c, to the HWHM of the seeing PSF, Δ. The ratio r_c/Δ for each galaxy is tabulated in Table 1 is and plotted in Figure 1 as a function of the ratio of effective radii, R_e, to Δ; R_e is determined by fitting the profile of each galaxy with a de Vaucouleurs (1958) law between $3r_c$ and the end of the profile. This is done in response to Schweizer's (1979) arguments that, since de Vaucouleurs law profiles are often an excellent description of the envelopes of elliptical galaxies, perhaps they can also describe the cores when smeared out by seeing. The intrinsic core might be considerably smaller than the seeing, and the ultimate departure of the core from the centrally unphysical de Vaucouleurs law would be completely obscured.

As seen in Figure 1, all galaxies have apparent cores significantly larger than the seeing; r_c/Δ is greater than 1.7 for all

TABLE 1

OBSERVED AND DECONVOLVED CORE PARAMETERS

NGC	r_c (arc")	r_c' (arc")	I_0 ($R/\square$")	I_0' ($R/\square$")	Δ (arc")	Δ' (arc")	r_c/Δ	R_e/Δ	γ	Resolution Class
545	1.80	1.09±0.18	16.42	15.77±0.15	0.86	0.59	2.11	51	0.86	III
547	1.92	1.15±0.18	16.53	15.94±0.13	0.86	0.59	2.25	62	0.81	III
584	1.92	1.21±0.25	15.15	14.48±0.22	0.87	0.70	2.21	43	0.93	III
596	1.50	0.90±0.14	15.28	14.62±0.13	0.74	0.51	2.03	67	0.96	III
636	1.93	1.39±0.25	15.81	15.29±0.23	1.01	0.79	1.91	36	0.74	III
720	5.00	4.58±0.01	16.23	16.12±0.00	1.01	0.70	4.98	46	0.00	I
741	2.73	1.91±0.03	16.83	16.39±0.02	0.78	0.60	3.52	107	0.14	I
821	1.50	0.90±0.13	15.18	14.51±0.12	0.67	0.49	2.26	70	0.98	III
1052	1.76	1.08±0.18	15.15	14.47±0.16	0.82	0.59	2.15	75	0.87	III
1199	1.59	1.12±0.27	15.75	15.23±0.26	0.91	0.70	1.76	47	1.09	III
1395	2.83	1.86±0.12	15.70	15.33±0.05	0.81	0.60	3.52	67	0.47	I
1400	1.84	1.25±0.25	15.51	14.99±0.21	0.87	0.70	2.13	40	0.91	III
1407	3.71	3.21±0.07	16.08	15.93±0.02	0.84	0.60	4.44	110	0.17	I
1426	2.32	1.30±0.23	16.15	15.40±0.16	1.02	0.68	2.29	34	1.13	III
1439	1.61	1.05±0.11	15.92	15.11±0.18	0.96	0.68	1.69	65	0.84	III
1453	2.28	1.38±0.21	16.00	15.46±0.12	0.98	0.68	2.34	43	0.97	III
1600	4.26	3.73±0.09	16.94	16.81±0.02	0.69	0.60	6.17	63	0.19	I
1700	1.70	1.38±0.32	15.31	14.86±0.34	0.94	0.86	1.81	29	0.87	III
3379	2.62	1.66±0.07	14.84	14.41±0.04	0.89	0.60	2.96	51	0.38	I
4261	2.97	2.61±0.05	15.84	15.68±0.02	0.67	0.60	4.43	76	0.17	I
4365	2.99	2.33±0.02	15.66	15.42±0.02	0.79	0.60	3.81	139	0.08	I
4374	3.67	2.99±0.02	15.29	15.08±0.01	0.82	0.60	4.48	91	0.06	I
4406	2.72	1.84±0.06	15.43	14.90±0.05	1.09	0.65	2.50	89	0.27	II
4472	4.20	3.70±0.03	15.42	15.31±0.00	0.72	0.58	5.87	129	0.00	I
4552	2.12	1.25±0.08	14.86	14.24±0.06	0.92	0.55	2.32	42	0.48	II
4621	1.43	0.84±0.19	14.60	13.89±0.20	0.76	0.56	1.89	118	1.23	III
4636	4.13	3.24±0.17	16.32	16.13±0.03	1.01	0.84	4.09	217	0.34	I
4649	4.60	3.41±0.11	15.51	15.27±0.02	0.79	0.57	5.82	52	0.32	I
4742	1.51	0.97±0.22	14.48	13.77±0.24	0.85	0.60	1.78	30	1.07	III
5845	1.68	1.11±0.15	15.24	14.45±0.15	0.92	0.63	1.84	6	0.84	III
5846	3.07	2.51±0.14	16.31	16.15±0.05	0.80	0.63	3.86	156	0.36	I
6086	1.96	1.21±0.06	16.98	16.27±0.08	0.87	0.60	2.27	43	0.43	II
6702	1.45	1.04±0.20	16.22	15.70±0.23	0.85	0.70	1.71	23	0.89	III
6703	1.37	1.27±0.30	15.36	15.11±0.30	0.72	0.79	1.90	51	0.97	III
7052	2.65	1.70±0.12	16.63	16.24±0.04	0.81	0.60	3.29	89	0.52	I
7454	1.51	0.99±0.16	16.31	15.67±0.18	0.72	0.59	2.10	57	0.88	III
7457	1.53	1.10±0.23	16.73	16.21±0.25	0.80	0.70	1.91	261	0.98	III
7562	2.01	1.20±0.15	16.03	15.38±0.13	0.88	0.59	2.28	45	0.68	III
7619	1.88	1.25±0.08	15.68	15.13±0.07	0.74	0.60	2.54	47	0.49	II
7626	1.78	1.11±0.04	16.04	15.37±0.07	0.84	0.65	2.13	77	0.41	II
7768	1.67	1.11±0.11	16.73	16.24±0.10	0.67	0.51	2.49	78	0.61	III
7785	1.90	1.12±0.21	16.17	15.63±0.17	0.85	0.59	2.25	37	0.99	III

NOTE.—Observed and deconvolved core parameters. Apparent core radii, r_c, central surface brightnesses, I_0, and seeing radii (PSF semimajor axis length), Δ, are listed. Primes mark deconvolved parameters. Errors in the deconvolved parameters reflect plausible uncertainties in the Wiener filter noise cutoff. Other parameters listed include the size of the apparent core and effective radius relative to seeing, the sharpening parameter, γ, and the resolution classes.

galaxies and has a median value of 2.3. One-third of the galaxies have values of $r_c/\Delta \geq 3.0$ and are considered to have resolvable cores, as discussed below. If it were assumed naively that all galaxies had King-type cores, then the convolutions computed by Schweizer (1981*a*) and Djorgovski (1983) would imply that all the program galaxies have intrinsic cores at least comparable to or larger than Δ. The deconvolved cores, however, are almost always smaller than the estimates based on King model convolutions. Furthermore, two suspicious features in Figure 1 discourage the interpretation that most of the galaxies have resolvable cores. First, many of the galaxies are clustered around values of $r_c/\Delta \approx 2$, creating an edge in the lower left-hand corner of the diagram. Such an edge would naturally be expected if the cores of the smallest core galaxies were largely due to seeing. Second, when the coreless de Vaucouleurs law profiles are convolved with seeing, the resulting apparent core radii, r_d, can be quite large. A plot of the r_d/Δ values for typical seeing-convolved de Vaucouleurs laws in the diagram shows that r_d can be larger than 3Δ for the largest values of R_e/Δ; indeed, even for the lower values of R_e/Δ, the purely seeing-induced de Vaucouleurs law cores are relatively larger than the cores of most of the observed galaxies. Without knowledge of the intrinsic structure of the galaxies, it is difficult to argue on the basis of r_c/Δ alone that the galaxies with the smaller values of r_c/Δ are resolved.

To explore further the possibility that the observed profiles might be explained simply as seeing-convolved de Vaucouleurs law profiles, comparisons were made between the observations

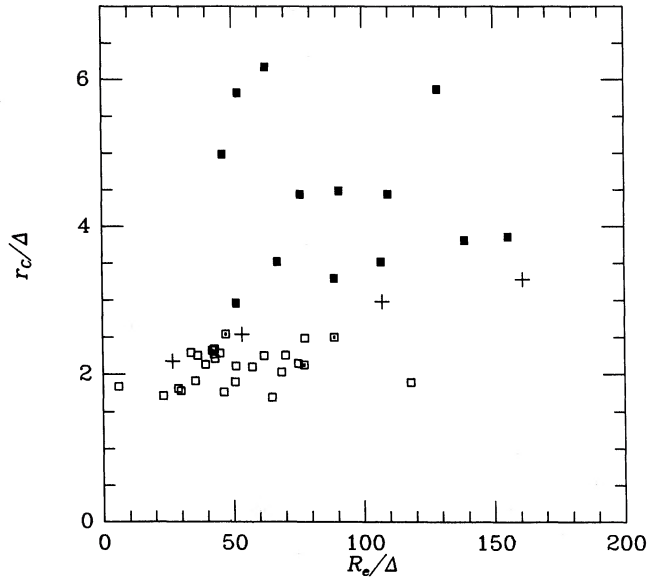

FIG. 1.—Apparent core radii plotted against effective radii, both scaled by seeing. Solid squares represent resolution class I galaxies, partially filled squares represent class II galaxies, and open squares represent class III galaxies. Large crosses represent various de Vaucouleurs models convolved with typical seeing.

and model profiles measured from two-dimensional de Vaucouleurs laws fitted to the galaxy envelopes (as described above), and then convolved with the observed seeing. As can be seen in Figures 2–4, the de Vaucouleurs laws are often an excellent match to the envelopes of the galaxies. No fits match the cores within the accuracy of the photometry and seeing convolutions established in Paper I, however. All galaxies with r_c smaller than r_d rise above the de Vaucouleurs laws in the center. On the other hand, all galaxies with $r_c/\Delta \geq 3.0$ have cores significantly larger than their corresponding seeing-convolved de Vaucouleurs laws. The galaxies with the largest values of r_c/Δ, NGC 1600, NGC 4472, NGC 4649, and NGC 720, have cores over 0.5 mag dimmer than the de Vaucouleurs comparisons. Most of the rest of this group have cores which at first rise above the de Vaucouleurs law and then flatten off and fall below it. NGC 1407 and NGC 4374 are good examples of this type. The conclusion is that galaxies with $r_c/\Delta \geq 3.0$ have intrinsically large cores which have been resolved under the present seeing conditions. Fourteen galaxies in the sample meet this criterion and thus comprise resolution class I, or the subset of galaxies with resolved cores. Further, eight class I galaxies have $r_c/\Delta \geq 4.0$, and thus appear to be extremely well resolved.

c) *Core Resolution and Deconvolution*

The cores of the class I galaxies also appear to be well resolved on the basis of their response to seeing-deconvolution. The median decrease in core radius after deconvolution for this class is just a modest factor of 1.27, and the deconvolved core radii are not strongly dependent on the limiting resolution set of the deconvolution. The resolution of the deconvolved core is set by the noise cutoff in the Wiener filter, which implicitly sets the size of Δ'. A well-resolved core should be insensitive to the final value of Δ', while an unresolved core should continue to sharpen as Δ' decreases. An important question, then, is how much sharpening is still taking place at the scale defined by the Wiener filter. To quantify this concept, the parameter γ is introduced, where γ is defined as the logarithmic slope of r_c' as a

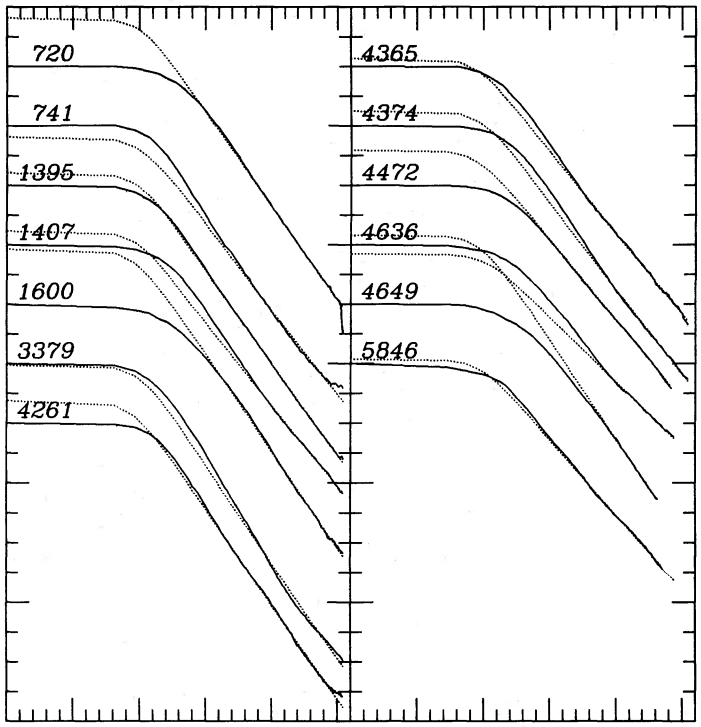

FIG. 2.—Observed surface photometry profiles of the resolution class I galaxies (*solid lines*) with seeing-convolved de Vaucouleurs models fitted to their envelopes (*dotted lines*). Vertical tick marks are in increments of 0.5 mag. The horizontal scale is isophote semimajor axis length π to the 0.25 power. Large tick marks are increments of $0.5(\pi)^{0.25}$. NGC 7052 had photometry of limited radial extent, and is not shown.

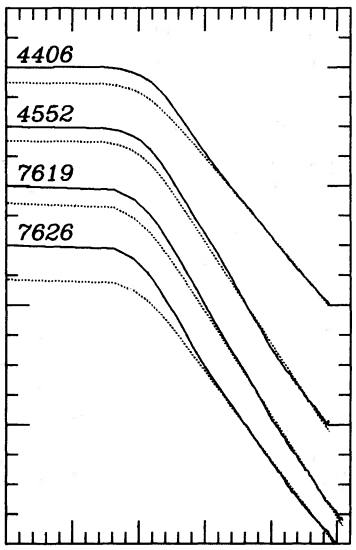

FIG. 3.—As in Fig. 2 for the resolution class II galaxies. NGC 6086 had photometry of limited radial extent, and is not shown.

function of Δ' at the point of optimal deconvolution. In practice, γ is measured from the relation

$$\left(\frac{r'_c}{r'_2}\right) = \left(\frac{\Delta'}{\Delta'_2}\right)^{\gamma}, \quad (4)$$

where r'_2 and Δ'_2 are the values of r'_c and Δ' obtained by performing the deconvolution with the noise level assumed to be twice as high as the originally estimated level. Typically, Δ'_2 is 14% larger than Δ'.

The γ-value for each galaxy is tabulated in Table 1 and plotted in Figure 5 as a function of r_c/Δ. As can be seen, γ is close to unity for most of the galaxies with small r_c/Δ, which means that their deconvolved core radii depend strongly on the final value of Δ'. On the other hand, γ decreases roughly as $(r_c/\Delta - 1)^{-1}$ over the sample, and has a median value of only 0.19 for the class I galaxies. For these galaxies, r'_c is fairly insensitive to the final values of Δ', which bolsters their designation as galaxies with resolved cores. It should be noted that only two galaxies, NGC 720 and NGC 4472, have $\gamma = 0$, which could be taken to mean that all other galaxies are unresolved, as their cores continue to sharpen to some degree as Δ' is decreased. Deconvolution tests on King models, however, show that γ can still be slightly different from zero when the deconvolved core is only slightly larger than the intrinsic core. Further, if the deconvolution is pushed past the estimated noise level, noise in the profile can cause the formal measurement of the core radius to shrink even below the intrinsic value. With these considerations, the small values of γ for the class I galaxies are taken to represent the uncertainty in the final values of r'_c rather than as an indication that the true cores could be much smaller. The adapted errors in r'_c listed in Table 1 are simply the change observed in each galaxy's r'_c in going from Δ'_2 to Δ'.

The use of the γ parameter may aid in the identification of a few more galaxies which may be nearly resolved. As seen in Figure 5, all galaxies in class I have $\gamma \leq 0.5$. Five galaxies with $r_c/\Delta < 3.0$ also have γ-values in this range. Since King models

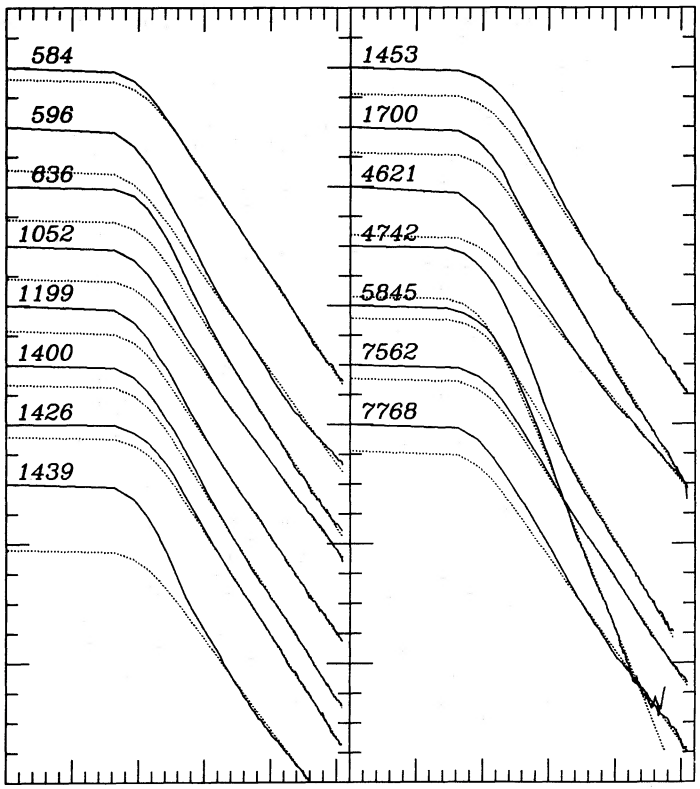

FIG. 4.—As in Fig. 2 for the resolution class III galaxies. No fits are shown for NGC 545, NGC 547, NGC 821, and NGC 7785, which had photometry of limited radial extent, and NGC 6702, 6703, NGC 7454, and NGC 7457, which were poorly described by de Vaucouleurs laws.

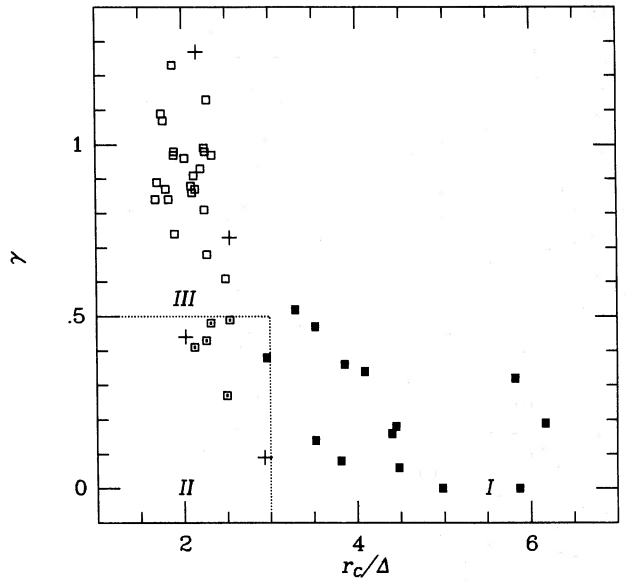

FIG. 5.—Sharpening parameter, γ, as a function of relative core radius. Symbols for the galaxies are as in Fig. 1. Dotted lines show the resolution class boundaries. Crosses in the class II section were derived from King model deconvolution tests; crosses in the class III section were derived from the de Vaucouleurs model deconvolution tests (see Paper I).

with intrinsic cores roughly equal to the seeing radius fall into this region of the diagram (these are plotted as large crosses in the lower left-hand portion of Fig. 5), these galaxies may also have intrinsic core radii nearly equal to Δ. It could be argued that some galaxies should have intrinsic cores in this size range, since there should be some transition objects between those that have completely resolved and those that have completely unresolved cores. Further, the deconvolution tests on the coreless de Vaucouleurs law galaxies show them to have $\gamma > 0.7$, in contrast to the behavior of the King models (these are plotted as large crosses in the upper left-hand portion of Fig. 5). With these considerations, resolution class II is defined to contain those galaxies which cannot readily be considered to be resolved by the r_c/Δ criterion, but which resemble the better resolved galaxies in their response to deconvolution. Specifically, class II contains those galaxies with $r_c/\Delta < 3.0$ and $\gamma < 0.5$. These galaxies are not considered to be completely resolved by the present study, but the true values of their core radii may be within 75% of their r_c' values by analogy with deconvolution tests on King models.

Last, resolution class III contains all galaxies which do not appear to have resolved cores based on either r_c/Δ or γ; specifically, class III contains all galaxies with $r_c/\Delta < 3.0$ and $\gamma > 0.5$. For most class III galaxies, $\gamma \approx 1$, which means that observations would have to be obtained with the seeing radii much smaller than the values of Δ' before their cores could be resolved. In general, this means that sub-arcsecond seeing conditions would be required. The extreme example of a class III galaxy is NGC 4621, which has $r_c' = 0''.84$ and whose deconvolved luminosity profile shows no sign of flattening except in the value of the central intensity.

IV. ANALYSIS

a) Core Profiles of Resolved Galaxies

The form of the core surface brightness profiles of the resolved galaxies provides useful information on their dynamics and structure. Although a complete investigation of these topics requires high-resolution velocity dispersion profiles, and is hence beyond the scope of the present study, a careful examination of the deconvolved surface brightness profiles has been carried out to look for features common to the cores of the resolved galaxies.

The initial course was to compare the cores of the resolved galaxies to the isothermal cores of King models of various concentrations. (The models were kindly provided by Kap-Soo Oh.) None of the galaxies could be fitted accurately by any of these models, however. The basic problem with the King model cores is that they are too abrupt in curvature; the transition between the flat center of the King profiles and their power-law envelopes takes place at radii within a factor of 2 of the formal core radius. To quantify this difference, first and second logarithmic derivatives have been calculated at the core radii of the galaxies based on the surface brightnesses at their core radii and at radii a factor of 2 inside and outside. By using an approximate form for the King models, $I(r) = (a^2 + r^2)^{-1}$, it is seen that both derivatives at the core of the King models are equal to -1, whereas the average first derivative (or power-law slope) at the cores of the resolved galaxies is found to be -0.79 ± 0.02, and the average second derivative (a measure of the curvature of the cores) is found to be only -0.48 ± 0.04. (Errors given in this section are errors in the mean unless noted otherwise.)

NGC 4472 is presented as a typical example of the poor agreement of the resolved galaxies with King models. The deconvolved profile of NGC 4472 is plotted in Figure 6 against a concentration 2.54 King model. The two profiles agree interior to the core but quickly diverge to over 0.5 mag outside. A different choice of radial scaling would improve the model fit to the inner envelope of the galaxy, but only at the expense of the present match interior to the core. NGC 4472 is interesting, since King (1978) and Kormendy (1982) identify it as a galaxy that is *well* described by a King model. Further, Kormendy also describes NGC 3379, NGC 4261, NGC 4365, NGC 4374, and NGC 4649 as having King-like isothermal cores; the

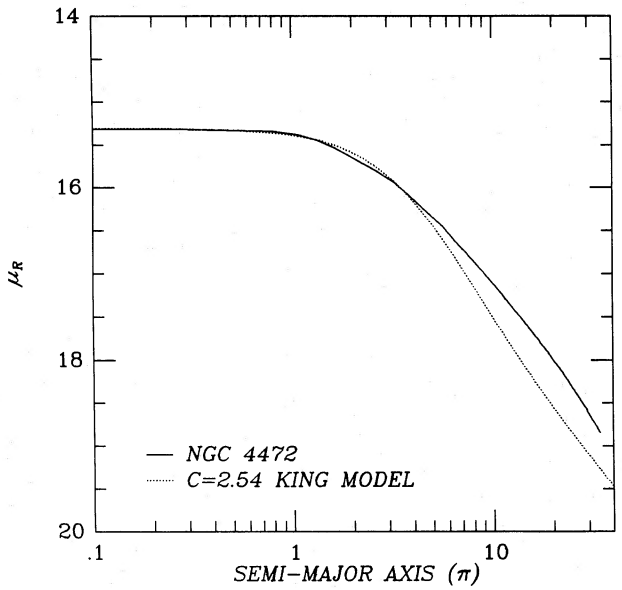

FIG. 6.—Concentration 2.54 King model fitted to the deconvolved core of NGC 4472.

disagreement between this study's and Kormendy's analysis of the core profiles is likely due to the previously identified differences in the surface photometry (see Paper I) for some of the galaxies (i.e., NGC 4261, NGC 4365, and NGC 4649) and differences in the seeing corrections for the remainder.

The failure of King models to describe the surface brightness profiles of the resolved galaxies is not surprising. King models were originally derived only to describe tidally truncated globular clusters (King 1966); their application to elliptical galaxies is on less theoretically sound bases. King models are computed on the assumption that the stellar velocity field is isotropic and isothermal and truncated at high energies. It is also assumed that the mass-to-light ratio is constant throughout the model. In light of the difficulties in fitting King models to the seeing-deconvolved galaxies, it is clear that at least one or more of these assumptions must break down. Recourse to more detailed and physically realistic models is required in order to explain the observed core structure.

A well-known example of a nonisothermal core is provided by the high-resolution profile of M87 of Young *et al.* (1978). Interestingly, half of the resolved galaxies could be scaled to fit M87 over almost their entire radial range. Further, most of the remaining resolved galaxies could at least be fitted to the inner envelope of M87. Because M87 is one of the very few elliptical galaxies with both a high signal-to-noise ratio and a high-resolution profile (prior to Paper I), it has served as a testing ground for a number of dynamical studies. Young *et al.* themselves attempted to explain the nonzero surface brightness gradient in the core of M87 as the response of a stellar system to the presence of a massive black hole. Other investigators (see Duncan and Wheeler 1980; Binney and Mamon 1982) have attempted to explain the core of M87 as the result of a non-isotropic velocity field. In the absence of high-quality surface photometry for a larger sample of elliptical galaxies, however, it was not known how common the structure of M87 was; the current study suggests that the central dynamics and structure of M87 may be typical of many elliptical galaxies.

The galaxies which match M87 well are NGC 720, NGC 741, NGC 1407, NGC 1600, NGC 4261, NGC 4374, and NGC 4649. The average power-law slope for the seven galaxies is -0.83 ± 0.04, as compared with -0.88 for M87; the average second derivative at their cores is -0.60 ± 0.04, as compared with -0.65 for M87. An average surface brightness profile of these galaxies, generated from each of their individual deconvolved profiles scaled to give the best match to M87, is plotted in Figure 7 against the Young *et al.* (1978) V profile of M87. The average profile matches M87 to within 0.04 mag from 2".5 in radius out to 40". Most of the individual profiles also fit M87 this well, although NGC 741 and NGC 1600 begin to depart from M87 (residuals greater than 0.05 mag) at about 4–5 core radii away from their centers.

The inner scale marks the radius at which the central nuclear spike of M87 begins to appear; since none of the current galaxies are seen to have such a spike, this region is ignored in the profile comparisons. Further, since M87 has a core of large angular size (8".35 based on fits of the current galaxies), this inner region corresponds to only 1" or so in the current galaxies. The current galaxies become fairly flat at this scale and, when extrapolated into the center of M87, fall below the inward extrapolation of the structural models of both Young *et al.* (1978) and Binney and Mamon (1982). This would imply that there is more light in the central nuclear spike than the above investigators have concluded, provided that the average profile can be used to represent the central structure of M87.

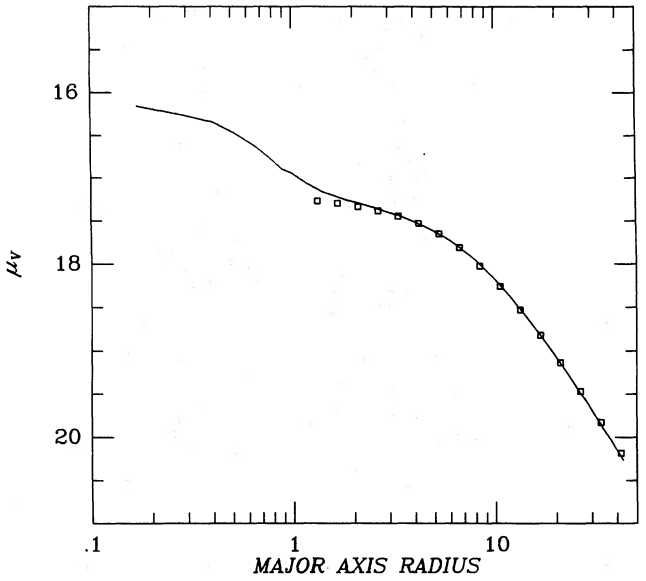

FIG. 7.—The squares represent a composite resolved profile generated from deconvolved profiles of NGC 720, NGC 741, NGC 1407, NGC 1600, NGC 4261, NGC 4374, and NGC 4649, scaled to a common core radius and fitted to the Young *et al.* (1978) V-profile of M87 (*solid line*).

The remainder of the resolved galaxies, NGC 1395, NGC 3379, NGC 4365, NGC 4472, NGC 4636, NGC 5846, and NGC 7052, have even more gently curving cores than M87. The average power-law slope is -0.75 ± 0.01, and the average second derivative is only -0.38 ± 0.04. Typically, the profiles of these galaxies can be scaled to match the profile of M87 from roughly 6" on out, but rise above its core inside this point. Of these seven galaxies, NGC 1395, NGC 4365, NGC 4472, NGC 4636, and NGC 7052 have similar core profiles, and can be scaled in radius and intensity to match one another. The average profile of these galaxies, generated from the individual profiles scaled in radius to produce the greatest mutual agreement, is also compared with M87 in Figure 8. An examination

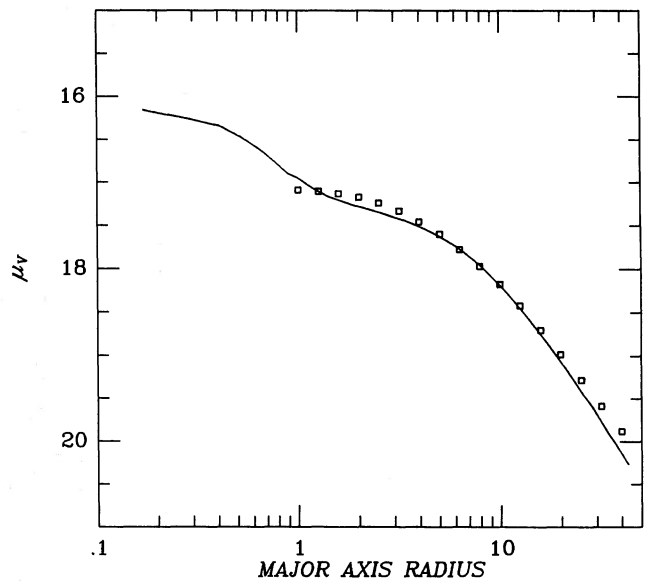

FIG. 8.—As in Fig. 7, but with a composite profile generated from NGC 1395, NGC 4365, NGC 4472, NGC 4636, and NGC 7052.

of the parameters derived from the sample of resolved galaxies turns up no clear difference between the the two sets of resolved galaxies other than in their ratios of effective radii to deconvolved core radii, R_e/r'_c. The former set of M87-like galaxies has an average $R_e/r'_c = 21 \pm 5$, while the latter set of five galaxies has $R_e/r'_c = 41 \pm 8$.

b) Nuclear Luminosity Spikes

The cores of the resolved galaxies were examined without success for the presence of central luminosity spikes similar to the one in M87. Figure 7 shows the central spike in M87 to be clearly visible as a distinct component superposed on the underlying core. None of the present galaxies has a central spike of such prominence, but precise upper limits are difficult to establish. By fitting the cores with various empirical models, it appears that the integrated magnitude of any nuclear spikes present in the galaxies are at least 2 mag dimmer than the central surface brightnesses of the galaxies; that is, the equivalent areas of any nuclear spikes are less than 0.16 arcsec^2. This limit is not particularly interesting, however, since it still allows an aggregate composed of several tens of globular clusters to remain undetected at the nuclei of the resolved galaxies.

A brief mention is made of two galaxies, NGC 1600 and NGC 4649, which may have nuclear spikes close to the limit of detectability. Three separate observations of NGC 1600 showed a subtle luminosity gradient in the inner 1″ of its surface brightness profile. Unfortunately, this galaxy has a very low central surface brightness and hence has a noisier profile than most. Furthermore, the apparent spike did not survive the reconstruction and deconvolution process. NGC 4649 shows a subtle inflection in its surface brightness profile 1″.5 away from its center, which is accompanied by an increase in isophote ellipticity and change in position angle inward of this radius; this inflection is enhanced by the deconvolution procedure.

c) Observational Parameters of the Sample

The observational parameters for the galaxies in the present sample are presented in Tables 2 and 3. Distances were derived using the $\gamma = 2$ Virgo infall model of Schechter (1980), assuming an infall velocity of 300 km s^{-1} and a Virgo distance modulus of 30.98 (Mould, Aaronson, and Huchra 1980); this choice of parameters implies a far-field Hubble constant of 84 km s^{-1} Mpc^{-1}. Where possible, the velocities of the individual galaxies were taken to be the average velocities of their groups. The bulk of the group assignments comes from either the Center for Astrophysics (CfA) survey of Geller and Huchra (1983) or the nearby (NB) group survey by the same investigators (Huchra and Geller 1982). Group identifications enclosed in parentheses represent ad hoc membership determinations not made by these investigators, but based on other references (see note to Table 2). The distances for the remaining galaxies are based directly on their radial velocities as given by Huchra *et al.* (1983), Sandage and Tammann (1981), and the RC2 (de Vaucouleurs, de Vaucouleurs, and Corwin 1976).

Parameters pertaining to the de Vaucouleurs effective radii of the galaxies are given in Table 3. The effective radii and surface brightnesses at the effective radii are derived from fits described in § III*b*. Both parameters are accurate to 10% but are more uncertain in galaxies with profiles that are of limited extent or are poorly described by a de Vaucouleurs law.

d) Central Mass-to-Light Ratios

Central mass-to-light ratios have been calculated for each galaxy, using the standard formula for a spherical core with an isotropic velocity field (King and Minkowski 1972):

$$\frac{M}{L} = \frac{9\sigma^2}{2\pi G I_0 r_c} . \tag{5}$$

The ratios were reduced to *blue* light by using an average $B-R$ value of 1.8 for the sample, and the absolute B-magnitude of the Sun was taken to be +5.48 (Allen 1973). Externally, the current mass-to-light ratios are generally in excellent agreement with those of Schechter (1980) when scaled to $H_0 = 50$ km s^{-1} Mpc^{-1}. Differences between this and Schechter's study are due largely to the assumption of diifferent distances of the galaxies relative to the Virgo Cluster.

An analysis of the mass-to-light ratios will be given later, but a discussion of their errors is presented here. The assumption of a spherical core shape is clearly wrong for some galaxies, but, as has been shown by Schechter (1980), ellipticity corrections to the mass-to-light ratios are modest for even the most flattened galaxies, and would be expected to average out to unity, since the galaxies are viewed at various inclinations. A more serious objection is the assumption of isotropic velocity fields in the cores. Since many of the resolved galaxies have M87-like core profiles, they may have significantly radially anisotropic velocity fields (see Binney and Mamon 1982). In this case the central velocity dispersions represent more a measure of the *total* velocity dispersion averaged along the line of sight than a measure of just one of the dispersion components, which are each a factor of $\sqrt{3}$ smaller than the total dispersion in the isotropic case; the calculated mass-to-light ratios would then be erroneously large. Since the mass-to-light ratios of the resolved galaxies vary only over a factor of 2, varying amounts of radial anisotropy could account for all or most of the observed scatter. Unfortunately, in lieu of high-resolution dynamical observations, the anisotropy of the central velocity fields cannot be estimated.

Brief mention is also made of the accuracy of the mass-to-light ratios of the unresolved galaxies. Although the final core radii and central surface brightnesses of the resolution class II and class III galaxies are only upper limits to their intrinsic values, their product, $I_0 r_c$, is fairly insensitive to seeing (see below), in agreement with the convolution experiments of Schweizer (1979). The median increase of $I_0 r_c$ after seeing deconvolution for the class III galaxies was only a factor of 1.14. The mass-to-light ratios for class II and class III galaxies may therefore be very close to their intrinsic values. On the other hand, Schweizer (1981*a*) has pointed out that if the cores are still *severely* unresolved, the measured $I_0 r_c$ products may be too small by factors of 2 or larger, in which case the derived mass-to-light ratios would be too large.

The last column in Table 2 lists the central B band luminosity density in solar units, which, as discussed below, appears to be an important parameter for determining the morphology of the cores. The luminosity densities are calculated from the core parameters by the formula (Peterson and King 1975)

$$\rho_c = \frac{I_0}{2r_c} . \tag{6}$$

e) Analysis of the Core Parameters

The picture presented by an analysis of relationship between luminosity L, r_c, and I_0, is that L and ρ_c are two independent parameters which determine the relationship between the core and the global properties of the galaxy. This analysis is outlined below.

TABLE 2

OBSERVATIONAL PARAMETERS

NGC	Group	Resolution Class	D (Mpc)	$-M_B$	r_c' (pc)	I_0' (R/□")	σ (km/s)	M/L_B	ρ_c Log L pc^{-3}
545	CfA 15	III	57	21.11	300	15.77	255	13	1.01
547	CfA 15	III	57	20.54	316	15.94	295	19	0.92
584	NB 45	III	19	20.21	111	14.48	230	9	1.96
596	NB 45	III	19	19.73	83	14.62	180	8	2.03
636	NB 45	III	19	19.19	128	15.29	186	10	1.58
720	(NB 45)	I	19	20.24	422	16.12	240	11	0.73
741	CfA 23	I	56	21.58	519	16.39	309	19	0.53
821	···	III	19	19.79	84	14.51	210	10	2.07
1052	NB 44	III	14	19.35	75	14.47	207	10	2.14
1199	···	III	31	20.02	166	15.23	208	9	1.49
1395	NB 32	I	16	19.89	143	15.33	245	17	1.51
1400	(NB 32)	III	16	19.06	96	14.99	277	23	1.82
1407	NB 32	I	16	20.37	247	15.93	288	23	1.04
1426	NB 32	III	16	18.72	100	15.40	163	11	1.64
1439	NB 32	III	16	18.59	81	15.11	182	13	1.85
1453	NB 47	III	43	20.79	285	15.46	280	12	1.16
1600	···	I	49	21.44	890	16.81	342	20	0.13
1700	···	III	42	21.33	280	14.86	258	6	1.41
3379	CfA 68	I	10	19.76	77	14.41	227	11	2.15
4261	dV 46	I	31	21.13	392	15.68	321	14	0.93
4365	CfA 106	I	16	20.37	177	15.42	263	17	1.38
4374	CfA 106	I	16	20.80	228	15.08	292	12	1.41
4406	CfA 106	II	16	20.98	140	14.90	262	13	1.69
4472	CfA 106	I	16	21.67	282	15.31	317	14	1.23
4552	CfA 106	II	16	20.31	95	14.24	276	12	2.13
4621	CfA 106	III	16	20.30	64	13.89	227	8	2.44
4636	CfA 106	I	16	20.49	247	16.13	227	17	0.96
4649	CfA 106	I	16	21.18	260	15.27	361	19	1.28
4742	NB 41	III	16	18.97	74	13.77	110	2	2.42
5845	CfA 150	III	24	18.94	129	14.45	233	7	1.91
5846	CfA 150	I	24	20.79	292	16.15	255	19	0.87
6086	···	II	107	21.43	625	16.27	331	16	0.50
6702	···	III	56	20.72	280	15.70	200	8	1.07
6703	···	III	30	20.18	183	15.11	189	6	1.49
7052	···	I	56	21.75	459	16.24	···	···	0.64
7454	CfA 163	III	24	19.59	115	15.67	135	9	1.47
7457	···	III	14	19.24	73	15.72	128	14	1.65
7562	(CfA 166)	III	38	20.54	223	15.38	289	15	1.30
7619	CfA 166	II	38	20.98	232	15.13	304	13	1.38
7626	CfA 166	II	38	20.83	206	15.38	275	15	1.34
7768	CfA 173	III	87	21.86	467	16.24	260	13	0.63
7785	···	III	42	20.67	226	15.45	241	11	1.27

NOTE.—Core parameters reduced to physical units are given. Central mass–to–blue light ratios, M/L_B, and central R luminosity densities, ρ_c, are given in solar units. Deconvolved core parameters are used in all cases. Absolute magnitudes are calculated from B_T magnitudes given in the RC2, or Harvard magnitudes for galaxies without B_T magnitudes. Extinction corrections have been applied on a galaxy-to-galaxy basis from Burstein and Heiles (1984). Extinctions are also applied to the deconvolved central surface brightnesses, but are less important since the surface photometry is in the R color band. Velocity dispersions were kindly provided by Faber (1983) and represent a weighted average of all published dispersion measures and Faber's own unpublished observations. Distances were derived as described in the text. Some ad hoc group memberships were made for the present study as follows: NGC 720 was not listed as a member of NB 45 by Huchra and Geller (1982), but was included in de Vaucouleurs's (1975) group dV 33, which is equivalent to NB 45. This assignment is not critical, since there is only a 7% difference between the distance derived directly from the radial velocity of NGC 720 and the distance derived from the average group velocity of NB 45. NGC 1400 was assigned to NB 32 on the basis of its angular proximity to NGC 1407, although its radial velocity is several standard deviations less than the mean velocity of this group. As noted by Schechter (1980), however, both the velocity dispersion and the color of NGC 1400 are inconsistent with its being at the much smaller distance implied by its radial velocity. NGC 7562 was not listed as a member of CfA 166, but is included in this group by Davies *et al.* 1983. In agreement with Schechter (1980), NGC 4261 is taken to be a member of de Vaucouleurs's Virgo W group (dV 46) rather than a member of the Virgo Cluster (CfA 106 or NB 41), as suggested by Geller and Huchra (1983). The velocity dispersion of NGC 4261 is normal for the galaxy's luminosity if it is at the distance of dV 46, but is spuriously high if the galaxy is a member of Virgo. Galaxies identified as members of dV 46, and others near NGC 4261 on the sky, generally have radial velocities similar to that of NGC 4261 (which are only 1 standard deviation larger than the mean velocity of Virgo).

TABLE 3

MAGNESIUM AND EFFECTIVE RADIUS PARAMETERS

NGC	Mg_2	R_e (kpc)	I_e (M_R arcsec^{-2})	$\langle M/L_B \rangle$	ρ_e (log L pc^{-3})
545:.....	0.339	12.1	22.14	15.8	−3.14
547:.....	...	14.5	22.46	23.5	−3.35
584.....	0.286	3.4	20.25	7.9	−1.84
596.....	0.241	4.7	21.48	11.1	−2.46
636.....	0.287	3.3	21.36	14.9	−2.26
720.....	0.354	4.3	20.53	8.9	−2.04
741.....	0.323	22.5	22.74	21.5	−3.65
821:.....	0.312	4.4	21.01	13.8	−2.36
1052.....	0.330	4.3	21.14	11.7	−2.28
1199.....	0.310	6.2	21.42	10.4	−2.56
1395.....	0.323	4.2	20.89	13.3	−2.18
1400.....	0.326	2.6	20.83	25.4	−1.95
1407.....	0.345	7.0	21.73	23.6	−2.73
1426.....	0.264	2.7	21.13	11.5	−2.19
1439.....	...	4.8	22.41	25.9	−2.84
1453.....	0.331	8.6	21.50	14.7	−2.74
1600.....	0.334	10.4	21.25	14.5	−2.71
1700.....	0.268	5.5	20.43	7.4	−2.11
3379.....	0.330	2.1	20.09	10.8	−1.56
4261.....	0.340	7.6	20.97	13.4	−2.48
4365.....	0.340	8.3	21.61	15.0	−2.77
4374.....	0.330	5.7	20.71	11.8	−2.24
4406.....	0.318	7.4	21.30	12.6	−2.59
4472.....	0.337	6.1	20.63	11.9	−2.23
4552.....	0.350	2.9	20.14	12.0	−1.72
4621.....	0.349	6.8	21.12	8.7	−2.48
4636.....	0.341	16.7	22.63	14.2	−3.47
4649.....	0.375	3.1	19.54	11.0	−1.51
4742.....	0.184	1.9	20.34	3.4	−1.63
5845.....	0.321	0.6	18.08	5.9	−0.23
5846.....	0.347	14.5	22.18	13.6	−3.24
6086:.....	0.334	19.1	22.48	22.9	−3.47
6702:.....	0.265	5.3	20.86	6.8	−2.27
6703:.....	...	5.3	21.14	8.0	−2.38
7052.....	...	19.5	22.28	...	−3.40
7454:.....	0.211	4.8	21.63	6.9	−2.53
7457:.....	0.190	13.8	23.79	15.8	−3.86
7562.....	0.302	7.4	21.31	15.4	−2.59
7619.....	0.364	6.5	21.00	14.5	−2.42
7626.....	0.347	12.0	22.08	17.5	−3.11
7768.....	0.312	21.9	22.65	14.4	−3.60
7785:.....	0.302	6.2	20.90	8.7	−2.35

NOTE.—Magnesium and effective radius parameters. The Mg_2 indices were kindly provided by Sandra M. Faber (1983). The de Vaucouleurs effective radii and surface brightnesses were derived as explained in the text. Typical errors in these parameters are about 10%; however, the galaxies marked with colons are either poorly described by de Vaucouleurs laws or have surface brightness profiles of limited radial extent, and thus may have much larger errors in the present parameters. Average *global* mass-to-blue light ratios, $\langle M/L_B \rangle$ and the average R luminosity densities, ρ_e, are given in solar units.

Figure 9 shows a strong relationship between I_0 and r_c in the sense that large core radii imply low central surface brightnesses and vice versa; a fit to the class I galaxies shows $I_0 \propto r_c^{-0.88}$. Close examination shows a few interesting aspects of this relationship. First, the mean relation between I_0 and r_c does not appear to be dependent on the degree of core resolution. An analysis of class II and class III galaxies shows the deconvolution algorithm to couple the core parameters as $I_0 \propto r_c^{-1.09 \pm 0.23}$, as the width of the PSF is described. (The error in the exponent is the standard deviation.) Seeing effects therefore cause the galaxies to move along lines that are nearly parallel to the average relation; this means that the constant of proportionality between I_0 and r_c is fairly insensitive to seeing. It also appears that this constant of proportionality is related to intrinsic luminosity; at a given core radius, brighter galaxies

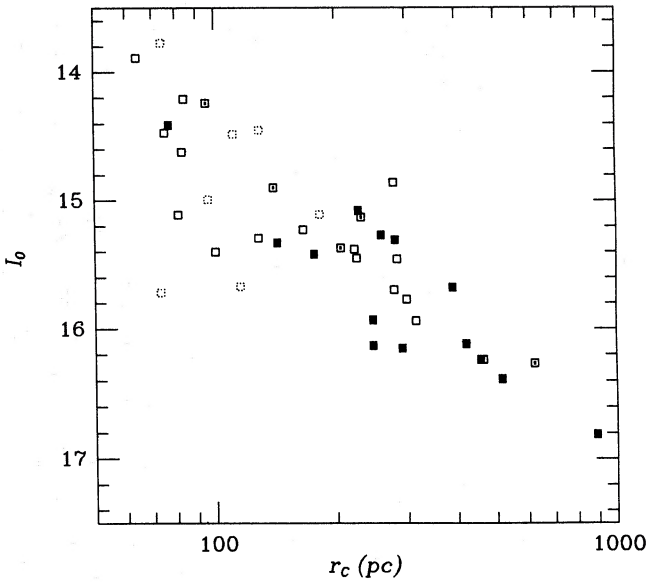

FIG. 9.—Deconvolved central surface brightness versus deconvolved core radius. Symbols for the galaxies are as in Fig. 1. Solid squares represent resolution class I galaxies, partially filled squares represent class II galaxies, and open squares represent class III galaxies. Broken squares represent class III galaxies not used in the analysis.

have higher central surface brightnesses. Distance errors could cause some of this effect, but its magnitude is fairly large; an increase of one magnitude in luminosity at a given core radius implies an increase in the central surface brightness of about the same amount. The effect is also visible in the Virgo Cluster galaxies, for which relative errors should be small.

Figure 10 shows L and r_c to be correlated (a fit to the class I galaxies gives $L \propto r_c^{0.84}$), although there is considerable scatter about the mean relation. NGC 720 and NGC 4621, for example, have about the same luminosity, but the core of NGC 4621 is at least 6 times as small as that of NGC 720. The scatter appears to be due to the relation between I_0 and r_c discussed

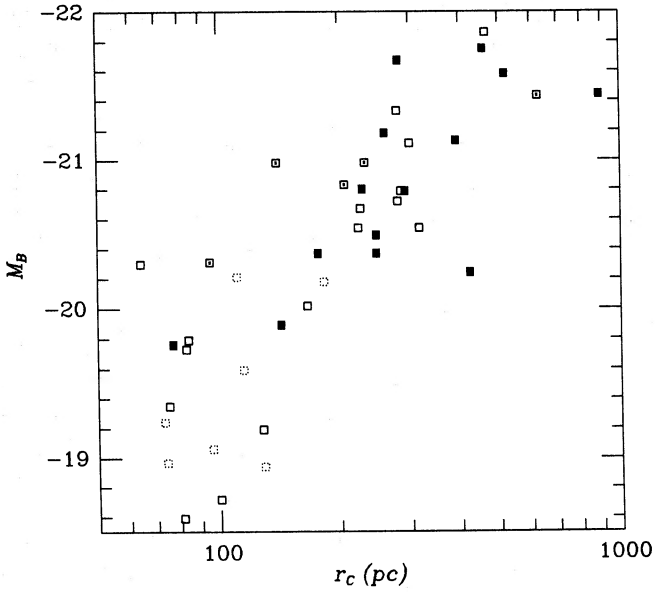

FIG. 10.—Total luminosity versus deconvolved core radius. Symbols for the galaxies are as in Fig. 9.

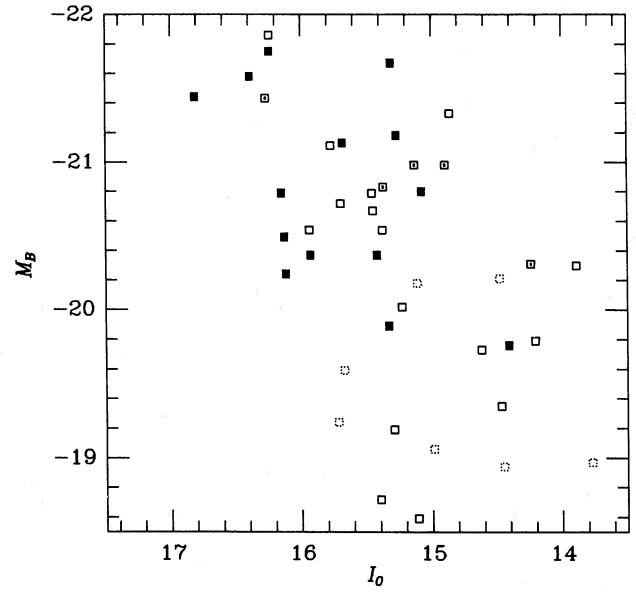

FIG. 11.—Total luminosity versus deconvolved central surface brightness. Symbols for the galaxies are as in Fig. 9.

above. At all luminosities, a smaller core is always associated with a higher central surface brightness. It is also interesting that class III galaxies generally have cores equal to or *smaller than* the resolved galaxies of the same luminosity. Since the class III core radii are really only upper limits, one would naively have expected them to be larger than the class I galaxies. In fact, the only galaxies that might be consistent with this picture are the low-luminosity galaxies in the lower left-hand corner of the figure. The scatter is intrinsic to the sample rather than due to seeing effects and must be accounted for. This point is reinforced by Figure 11, which plots L against I_0. The scatter in this diagram is even larger—it is difficult to see any relationship between the two variables at all. Again the scatter reflects the relationship between I_0 and r_c; at a given luminosity, a low surface brightness implies a large core.

The picture presented by the relations between L, r_c, and I_0 is that the parameters fall on a thin plane in their three-dimensional space. The plot of I_0 versus r_c, for example, appears to present an almost edge-on view of the plane, while the plot of L versus I_0 is almost a face-on view of the plane. To investigate this possibility, recourse was had to a principal component analysis (see Kendall 1975)). (The analysis package was kindly provided by J. Jesus Gonzales.) The result of this analysis is to confirm that the three variables fall on a plane, and to show that a highly significant second component is responsible for the placement of the galaxies within the plane.

The initial course taken was to perform the principal component analysis on only the class I galaxies. To examine the characteristics of the plane described by L, r_c, and I_0, pairwise plots were made of the principal components, K_1, K_2, and K_3. (Component plots of the final analysis adopted, which included σ as a fourth variable, are shown in Figs. 12 and 13.) K_1 and K_2 are orthogonal coordinates which map the distribution of the galaxies in the plane. K_3 describes the height of the galaxies above or below the K_1-K_2 plane; the thickness of the plane is not significant and presumably reflects observational errors. These plots showed that most class II and class III galaxies also fell on the plane defined by the class I galaxies, which implies that residual effects of seeing have little effect on the thickness of the plane. The next step was therefore to perform the analysis on all galaxies that appeared to be in the plane. (The galaxies excluded from the fit were the S0 galaxies NGC 584, NGC 5845, NGC 6703, NGC 7454, and NGC 7457, and

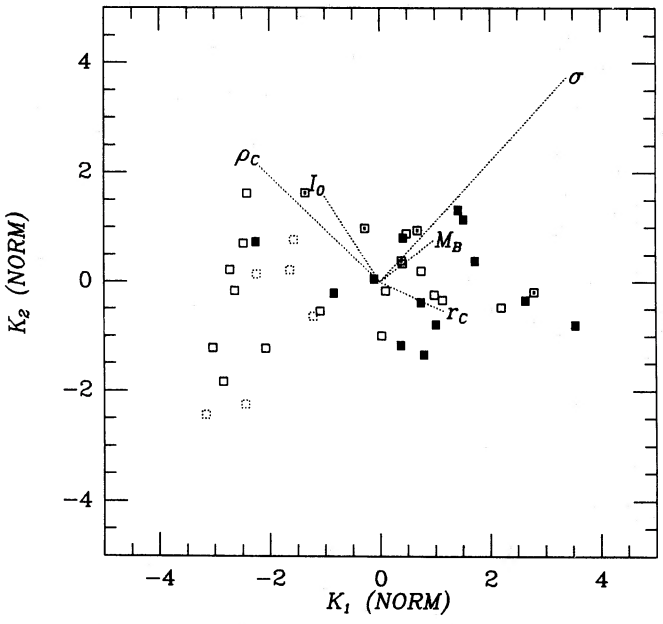

FIG. 12

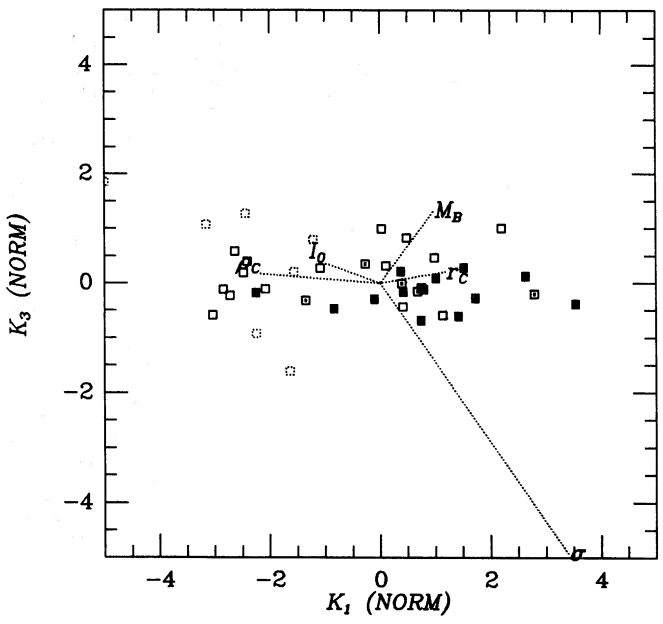

FIG. 13

FIG. 12.—Principal components K_1 and K_2 for the four-dimensional space described by r_c, I_0, L, and σ. Principal component are in logarithmic units. Input parameters are normalized to unit variances. Vectors (*dotted lines*) show the change in the component values produced by a factor of 4 increase in a given input. Symbols for the galaxies are as in Fig. 9.

FIG. 13.—As in Fig. 12, but with K_3 plotted instead of K_2

two ellipticals, NGC 1400 and NGC 4742.) The results of the analysis showed little change; the form of the plane containing L, r_c, and I_0 is

$$L \propto r_c^{2.43\pm0.11} I_0^{1.73\pm0.11} , \quad (7)$$

or, in terms of the observational parameters given in Table 2,

$$M_B = -6.08 \log r_c' + 1.73 I_0' - 33.07 . \quad (8)$$

Residual seeing effects in r_c and I_0 influence the right-hand side of the above equation only as $r_c^{1/2}$, given the coupling of the two parameters discussed above. The plane is also fairly insensitive to distance errors, since at any surface brightness L goes nearly as r_c^2. In passing, it is noted that there are two formal methods of performing principal component analysis, depending on whether or not the input parameters are normalized to have unit variances. Equations (7) and (8) were derived by using unnormalized data, but show little change when normalized data are used instead.

Once it has been determined that L, r_c, and I_0 form a plane with a significant second component, efforts were made to see how other observational parameters are related to these variables. When central velocity dispersion was added to the analysis, the form of the plane did not change, which means that two components were still sufficient to map the spread of points in the four-dimensional space. The vector in the plane describing the dependence of the principal components on velocity dispersion is found to be nearly parallel to the luminosity vector. This means that central velocity dispersion provides no more information about the core parameters than is already given by luminosity. Conversely, the core parameters are not found to have any bearing on the Faber and Jackson (1976) relation between velocity dispersion and luminosity, which for this sample is $L \propto \sigma^{4.38}$. Residuals in the Faber-Jackson relation are found to influence the thickness of the plane, but are uncorrelated with the preexisting insignificant third component, owing to scatter in the core parameters alone. As Terlevich *et al.* (1981) argue for the presence of a second parameter to account for residuals within the Faber-Jackson relation, the present analysis shows that this parameter would have to be orthogonal to the current plane, which means that elliptical galaxies may at least be a *three*-parameter family. Consistent with this, the central Mg_2 index also fails to provide any further information about the core parameters and appears to be related only to residuals in the Faber-Jackson relation, as was suggested by Terlevich *et al.*

f) Identification of the Principal Components with Physical Parameters

The conclusion from the principal components is that luminosity alone is insufficient to explain the variance in the observed core properties and that no further information on the core is given by central velocity dispersion or Mg_2 index. To identify the basic variables driving the placement of galaxies within the plane, the principal components were plotted against each other in Figures 12 and 13. The components shown are derived from an analysis of L, r_c, I_0, and σ (using normalized variables), including all galaxies except the ones noted above. The plot of K_1 versus K_2 represents a face-on view of the fundamental plane. Tracks are also plotted for each observational parameter, showing how the galaxies would move within the plane for a factor of 4 increase in a given parameter, with all other parameters remaining fixed.

The directions of the parameter vectors allow a plausible identification of the fundamental physical variables driving distribution of points in the plane. The plot of K_1 versus K_2 shows that tracks for both r_c and I_0 are nearly perpendicular to L; this suggests that the second component may be a linear combination of these two variables. An excellent candidate for the second component appears to be the central luminosity density, ρ_c. The vector for a change in ρ_c is also plotted in Figures 12 and 13, showing it to be nearly exactly perpendicular to the luminosity track, but also nearly parallel to the K_1-K_2 plane. A formal plot of ρ_c versus L (Fig. 14) is almost identical with the plot of K_1 versus K_2, but for a rotation of the axes. Since the axes are rotated, a general correlation exists between ρ_c and L, as can be seen in Figure 14; a formal fit finds $\rho_c \propto L^{-3.2}$. Despite this correlation, however, the large range in ρ_c at any given value of L naturally accounts for the scatter seen in the original relationships between the observational parameters and variations in the degree of core resolution of galaxies of the same luminosity and distance. NGC 720 and NGC 4621, for example, were identified above as having disparate core properties despite their similar luminosities; their central luminosity densities differ by at least a factor of 50.

With the use of ρ_c as a second parameter it is possible to rewrite core radius and central surface brightness as a function of both L and ρ_c. The relationships derived are

$$r_c \propto L^{0.24} \rho_c^{-0.42} , \quad (9a)$$

$$I_0 \propto L^{0.24} \rho_c^{0.58} , \quad (9b)$$

or, in terms of the parameters in Table 2,

$$r_c' = 311 \left(\frac{100}{\rho_c}\right)^{0.42} 10^{-(M_B+21)/10.4} \text{ pc} , \quad (9c)$$

$$I_0' = 22.27 + 0.24 M_B - 1.46 \log \rho_c \, M_R \text{ arcsec}^{-2} . \quad (9d)$$

The central mass-to-light ratios can also be written in terms of L and ρ_c. The analysis above shows that central velocity dispersion is related to L only (with the caveat noted below). The observed Faber-Jackson relation then implies that the lumi-

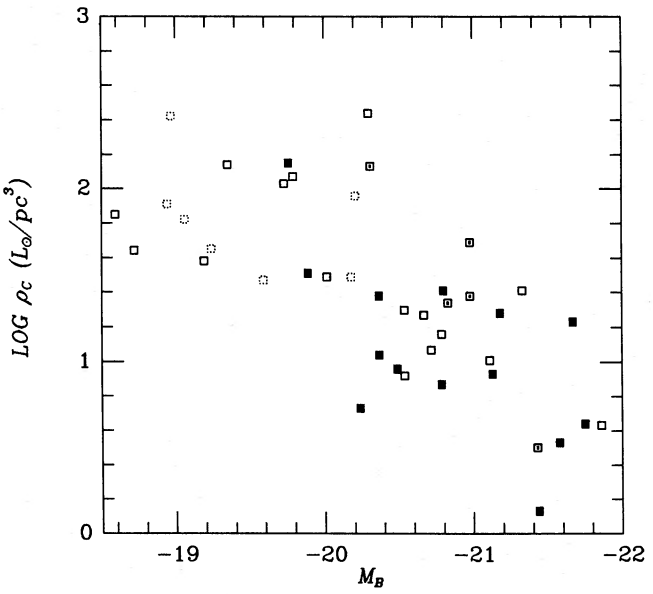

FIG. 14.—Deconvolved central luminosity density versus total luminosity. Symbols for the galaxies are as in Fig. 9.

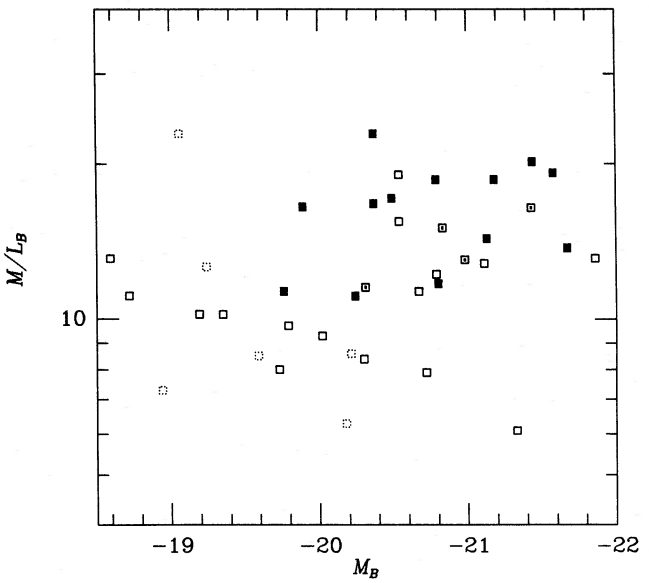

FIG. 15.—Central mass-to-light ratio versus total luminosity. Symbols for the galaxies are as in Fig. 9.

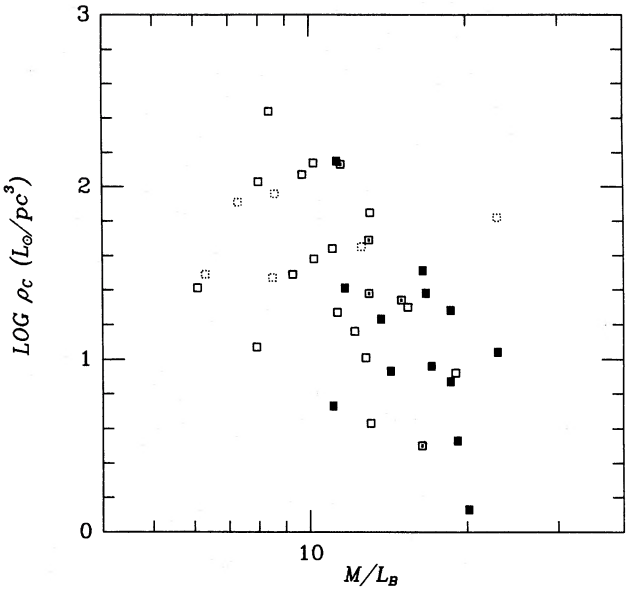

FIG. 16.—Deconvolved central luminosity density versus central mass-to-light ratio. Symbols for the galaxies are as in Fig. 9.

nosity contribution to M/L becomes insignificant, and that the mass-to-light ratios depend on central luminosity density only as

$$M/L = 19.4\rho_c^{-0.17}. \quad (10)$$

The above result is not strongly dependent on the exact slope of the Faber-Jackson relation; even if $L \propto \sigma^5$, the dependence of M/L on luminosity goes only as $L^{-0.08}$. This analysis is confirmed in Figures 15 and 16, in which M/L is plotted against L and ρ_c, respectively. Although there is considerable scatter, the plot of M/L versus ρ_c shows a much clearer correlation than is visible between M/L and L. A fit performed on the class I and class II galaxies shows $M/L_B = 22.6\rho_c^{-0.18\pm0.04}$, in excellent agreement with the relationship derived above (the larger constant of proportionality may be due to the stronger Mg_2 indices of these galaxies, as discussed below). The plot of M/L versus ρ_c also shows good discrimination between the resolved and unresolved galaxies; the observed central densities (which are highly sensitive to residual seeing) of the class III galaxies are generally lower than those of the resolved galaxies at a given mass-to-light ratio. Further, the class II galaxies fall among the class I galaxies in the diagram, which supports the conclusion that these galaxies may be nearly resolved.

The result that M/L does not depend on L is derived from both a direct comparison of the two quantities and an analysis of the parameters controlling the variables used to calculate M/L. Although Faber and Jackson (1976) observed $M/L \propto L^{0.5}$, later investigators (such as Schechter 1980 and Tonry and Davis 1981) found no evidence for any dependence of M/L on L. Other investigators have proposed various dependences of M/L on L based purely on combining the separate dependences of I_0, r_c, and σ on L, or metallicity effects (see Kormendy 1982 for a review). The present analysis shows that this approach is invalid, since it overlooks the effects of the second parameter, ρ_c, in controlling the morphology of the cores. When ρ_c is used to account for the "scatter" in the relationships of I_0 and r_c to L, the L dependence of these two quantities is different from that derived by assuming that L is the sole controlling parameter.

So far, this analysis has assumed that σ is completely specified by luminosity. Although this is true in terms of the other quantities used to calculate M/L, Terlevich *et al.* (1981) argued that the Mg_2 index provides additional information about σ. In this case, M/L should be correlated with Mg_2 in addition to ρ_c; such a relationship was initially found by Tonry and Davis (1981), who used global M/L ratios and a metallicity indicator based on Mg *b* and Na D line strengths, and was verified by Efstathiou and Fall (1983). This relationship is also confirmed here in Figure 17, which plots M/L versus the Mg_2 index. Since the above analysis found ρ_c to be independent of Mg_2, this result would imply that M/L is controlled by two separate

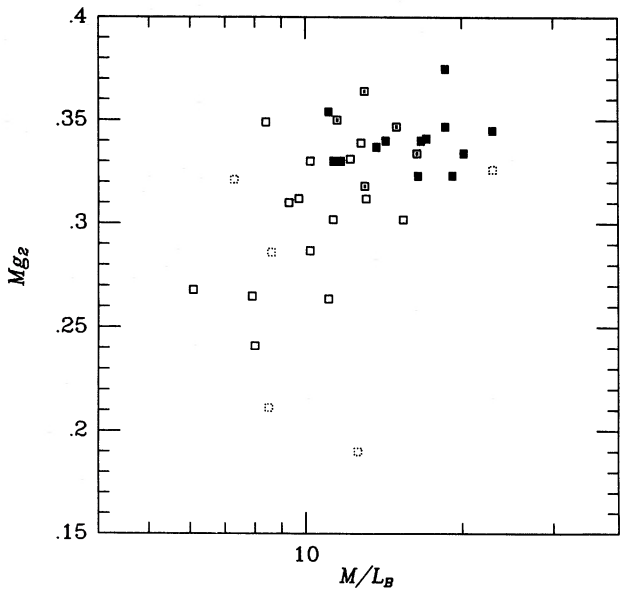

FIG. 17.—Mg_2 index versus central mass-to-light ratio. Symbols for the galaxies are as in Fig. 9.

parameters; adding in the dependence of σ on Mg_2 yields

$$M/L = 22.4\rho_c^{-0.17}10^{2.5(Mg_2-0.35)} . \quad (11)$$

Unfortunately, this relationship is difficult to verify directly. Since M/L is based on three separate observational parameters, observational errors are likely to cause much of the scatter seen. The scatter in M/L may also reflect anisotropic core velocity fields, as noted above.

In spite of these difficulties, it is worth considering a possibility raised by Efstathiou and Fall (1983) that M/L is the second parameter controlling the Faber-Jackson relationship. These investigators argue that metallicity may influence the stellar mass function, which in turn influences the mapping of σ onto luminosity. The present results suggest, via the present core luminosity density, that the stellar mass function may also have depended on the initial gas or cloud density in the core. In this case, M/L is controlled by more than one parameter, which could possibly account for Efstathiou and Fall's concern that M/L may not be uniquely related to the formal second parameter extracted by a principal component analysis on the Faber-Jackson relationship. The present analysis shows that, in the space defined by the core parameters, σ, and luminosity, the M/L axis will be projected onto the Faber-Jackson second-parameter axis, but will not be parallel to it. This is not surprising, since the Faber-Jackson second-parameter axis is perpendicular to the line defining the mean relation, while variations in M/L at a given luminosity will change the values of σ only. The formal identification of M/L as the second parameter is tricky, even when the assumptions used to calculate M/L are valid; since M/L is calculated from σ, random errors in σ at a given luminosity will naturally produce some of the corresponding variation in M/L.

g) *Comparison of Core with Global Parameters*

The principal result so far is that the core properties appear to be determined by a local quantity, central luminosity density, as well as a global quantity, total luminosity. The question that now arises is whether similar results can be obtained from an analysis of the global scale parameters of the galaxies. An answer to this question comes from performing a parallel analysis by substituting the effective radius for the core radius, and surface brightness at the effective radius for central surface brightness.

A principal component analysis performed on L, R_e, and I_e shows that these parameters also fall on a thin plane similar to that formed by luminosity and the core parameters; again, two components in the three-dimensional space are found to be significant. The specific form of this plane is found to be

$$L \propto R_e^{2.15\pm0.06} I_e^{1.36\pm0.06} , \quad (12a)$$

or, in terms of the parameters in Table 3,

$$M_B = -28.92 - 5.38 \log R_e + 1.36 I_e . \quad (12b)$$

To some extent, this relation is expected, as a de Vaucouleurs law fit produces a similar estimate of the luminosity, $L \propto R_e^2 I_e$. There is nothing inherent in the fitting procedure, however, which implies that these variables should form a plane with the existence of a significant second parameter; R_e and I_e could each be separately related to L only, for example.

An analysis of the form of the plane again leads to the identification of luminosity density as the second component, which in this case can be considered as an average luminosity density

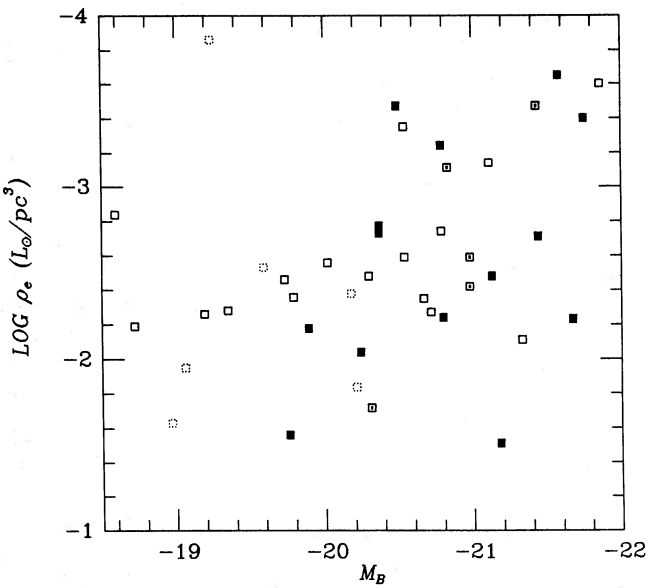

FIG. 18.—Average luminosity density versus total luminosity. Symbols for the galaxies are as in Fig. 9, however, resolution effects are unimportant, since effective radius parameters are used.

for the galaxy, ρ_e, where

$$\rho_e = \frac{I_e}{2R_e} . \quad (13)$$

In the present case, ρ_e appears to be much more independent of L than ρ_c, as can be seen in Figure 18. In terms of L and ρ_e, R_e and I_e can be expressed as

$$R_e \propto L^{0.28}\rho_e^{-0.39} , \quad (14a)$$

$$I_e \propto L^{0.28}\rho_e^{0.61} , \quad (14b)$$

or, in terms of the observational parameters,

$$R_e = 4.7(100\rho_e)^{-0.39}10^{-(M_B+21)/8.78} \text{ Kpc} , \quad (14c)$$

$$I_e = 23.25 - 1.53 \log \rho_e + 0.28 M_B M_R \text{ arcsec}^{-2} . \quad (14d)$$

Further, it is possible to define a global average mass-to-light ratio (Binney 1982), $\langle M/L \rangle$, where

$$\left\langle \frac{M}{L} \right\rangle = \frac{0.201\sigma^2}{GI_eR_e} , \quad (15)$$

on the assumption that the galaxy is well approximated by a de Vaucouleurs model of constant mass-to-light ratio. In terms of L and ρ_e, then,

$$\left\langle \frac{M}{L} \right\rangle = 24.2(100\rho_e)^{-0.23}10^{-(M_B+21)/36} . \quad (16)$$

As before, the mass-to-light ratio shows a clear dependence on ρ_e but a very weak or insignificant dependence on L. This is visible in Figures 19 and 20, which plot $\langle M/L \rangle$ versus L and ρ_e, respectively. When averaged over the entire sample, the global mass-to-light ratios are found to agree well with the core values; the average ratio of the core M/L to the global M/L is 0.99, with a standard deviation of 0.24. The class I galaxies alone, however, are found to have systematically higher core M/L values when compared with their global values, although the reason for this is not understood.

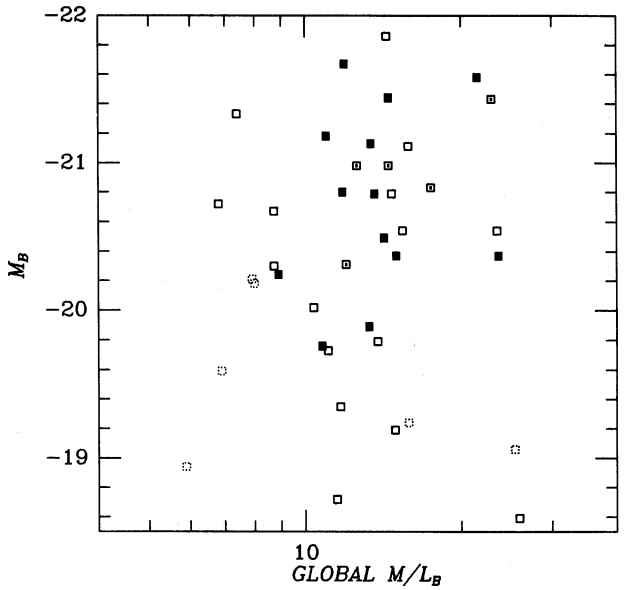

FIG. 19.—Total luminosity versus global mass-to-light ratio. The symbols for the galaxies are as in Fig. 9; however, resolution effects are unimportant, since effective radius parameters are used.

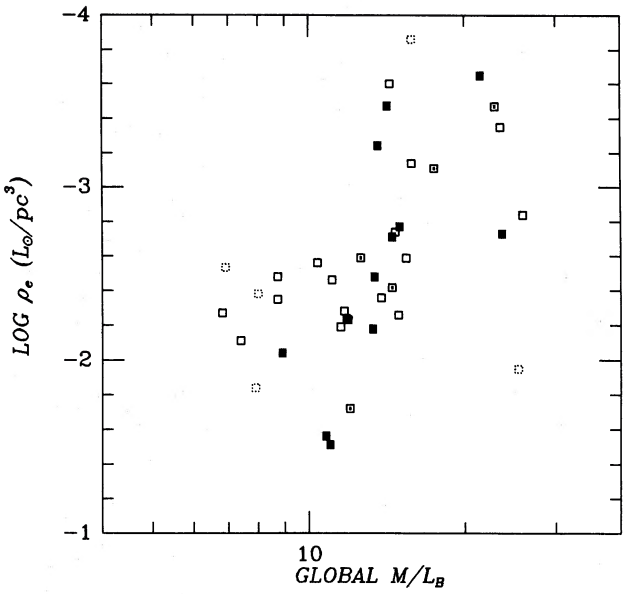

FIG. 20.—Average luminosity density versus global mass-to-light ratio. The symbols for the galaxies are as in Fig. 9; however, resolution effects are unimportant, since effective radius parameters are used.

The present analysis leads to the conclusion that both the average and core luminosity densities are largely independent of luminosity. How are these two quantities related to each other? By combining equations (9a) and (14a), it is seen that ρ_e/ρ_c depends only on R_e/r_c. A direct fit of these two ratios to each other shows

$$\rho_c = 7.3 \times 10^3 \left(\frac{R_e}{30 r_c'}\right)^{2.26} \rho_e^{1.02} . \quad (17)$$

This result is essentially independent of seeing, since from equation (9a), $\rho_c \propto r_c^{-2.38}$ for any given galaxy; the error in ρ_c from any error in r_c' thus preserves equation (17) (within the errors in the exponents). Interestingly, neither R_e/r_c nor ρ_e/ρ_c depends on luminosity. This is result is verified directly in the former case by Figure 21, which plots R_e/r_c versus L.

V. DISCUSSION

a) *Core Structure and Star Formation in a Protogalaxy*

The present study finds that although the central luminosity density of elliptical galaxies is roughly related to the inverse cube of luminosity, there is considerable scatter about the mean relationship, which means that central luminosity density is fairly independent of luminosity. The size and density of the core are also largely independent of the effective radius or average luminosity density of the galaxy. The formation of the core therefore is not uniquely determined by the formation of the envelope of the galaxy or by any identifiable global property of the galaxy. The core's independence of the rest of the galaxy is consistent with core formation by dissipational processes as suggested by Larson (1974*a*). Although Larson's modeling assumes that rotation is important in elliptical galaxies and is therefore at odds with more recent observational findings, the qualitative features of his models still offer useful insight into possible formation mechanisms of the core. In Larson's picture the core would not necessarily reflect the global properties of the galaxy but would rather depend sensitively on the history and mechanism of star formation as the initial protogalactic gas cloud was converted into stars.

Larson (1974*a*) proposes that the cores are formed out of gas left over from prior star formation in the envelope, which falls in and is accreted by the center of the galaxy. The final core density depends on how much gas is left after the formation of the outer envelope, and how much dissipation is allowed to take place. Under this picture, the growth of the core is limited by the onset of galactic winds produced by supernovae, which remove any leftover gas and hence "freeze in" the existing stellar density profile. The ability of supernovae to remove the gas depends on the depth of the galactic potential, which in turns is related to the total mass of the system; Larson predicts,

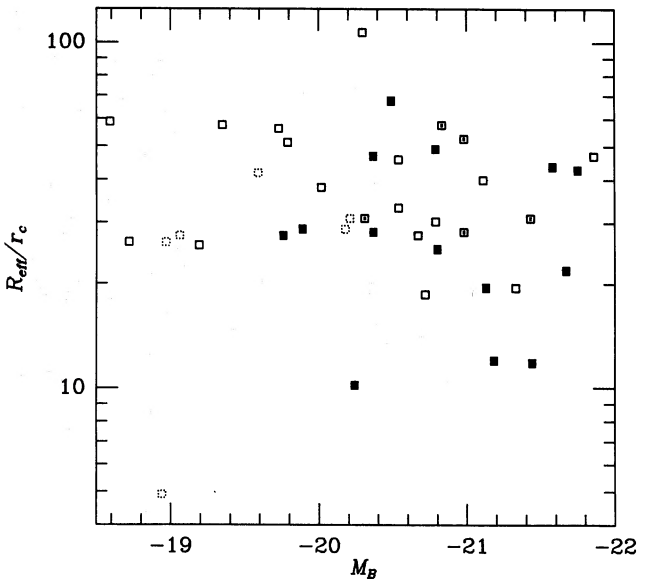

FIG. 21.—Ratio of effective radius to core radius versus total luminosity. Symbols for the galaxies are as in Fig. 9.

therefore, that the cores in more luminous galaxies should be more compact. Although this prediction is not verified by the present study, Larson's picture may still be valid if other mechanisms can control the amount of gas present in the forming protogalaxy. Tidal encounters or mergers during an early stage, for example, could remove or add more gas to the system; in fact, the present results may be most consistent with the formation of ellipticals by the successive mergers of gas clouds, as proposed by Tinsley and Larson (1979). The observed cores, therefore, would reflect random environmental conditions or interactions during the epoch of galaxy formation, rather than any global properties of the galaxies themselves. Another interesting aspect of Larson's models is that they often have the more shallow nonisothermal core profiles seen here, but with centrally depressed velocity dispersions, unlike M87 (Larson 1974*b*). Unfortunately, as noted in § IV*a*, high-resolution dynamical data are not available for the present sample to test this possibility.

The possibility that the formation of the cores is strongly dependent on the amount of gas left over from star formation in the envelope is especially appealing in the case of NGC 4621. As noted before, NGC 4621 has the largest central luminosity density in the sample (actually still a lower limit); it also has a weak stellar disk which extends from the core into the inner envelope (Lauer 1985*b*). The disk may be an example of the "incipient disk" seen in some of the models of Larson (1975), which arises only in the latest stages of star formation, when the leftover gas survives long enough to dissipate into a plane. Both the dense core and disk therefore may be associated with the survival of an especially large amount of gas from the initial burst of star formation in NGC 4621.

A dissipation picture for core formation also may account for the observed dependence of the mass-to-light ratios on the central luminosity density and central Mg_2 index. Since the central density in this picture depends directly on the amount of dissipation that took place, any sensitivity of the stellar mass function to the initial gas densities or temperatures might be reflected in the final relationship between luminosity density and mass-to-light ratio. Likewise, if the stellar mass function is influenced by metallicity, then the observed relationship between the Mg_2 index and the mass-to-light ratio might be explained if the stars in the core were formed well after the gas was already enriched by star formation in the envelope.

b) Core Structure and Mergers

It may be difficult to explain the observed core structure if elliptical galaxies were formed by any sort of purely hierarchical or cannibalistic merger scheme. Although the effects of mergers on the cores of elliptical galaxies are poorly understood, within the broad context of current work on this topic (see White 1982 for a review) it appears difficult to account for the lack of any correlation of R_e/r_c with luminosity and the large amount of scatter in the relationship between ρ_c and luminosity, if increasingly luminous elliptical galaxies are the end products of increasingly large numbers of mergers. *N*-body simulations of mergers of purely dissipationless stellar systems show that subsequent changes in the luminosity profiles of the objects are nonhomologous. The effective radius of the merger remnant is found to increase relative to some inner radius (such as the radius containing one-tenth the mass of the galaxy) when compared with the progenitors; basically it appears that stars in the envelopes of the merging galaxies bear the brunt of absorbing the pair's orbital energy. If dissipation were added, one might expect the core to become more concentrated, increasing the disparity between the behavior of the core and effective radius as more luminous galaxies were built up.

These nonhomologous effects are strongly visible in the merger simulations carried out by Farouki, Shapiro, and Duncan (1983) and Duncan, Farouki, and Shapiro (1983). In the first paper these investigators propose that increasingly luminous elliptical galaxies are built up in a sequence of mergers between increasingly larger stellar systems; in the second paper they consider the case in which an elliptical galaxy grows by repeatedly eating small systems. In both cases, their *N*-body simulations show that R_e/R_{10}, where R_{10} is the one-tenth mass radius, increases strongly with luminosity. If their result that r_c decreases (and ρ_c increases) with luminosity in the hierarchical scenario is correct, then R_e/r_c would be an even stronger function of luminosity. Further, Farouki, Shapiro, and Duncan (1983) find that the average luminosity density decreases with luminosity, which means that it would be anticorrelated with central density. These relationships are strongly at odds with the results presented here.

The behavior of the core itself in mergers is highly uncertain. As noted above, Farouki, Shapiro, and Duncan (1983) suggest that the core of the merger remnant of two identical stellar galaxies can actually *decrease* in size and increase in density, although the resolution of their models is poor in the core. Villumsen (1982), on the other hand, uses a more sophisticated *N*-body code in studying the mergers of identical galaxies and suggests that the core does become more diffuse. Kormendy (1984) discusses the more general problem of heterogeneous mergers of elliptical galaxies and uses simple physical arguments to show that the dense core of a low-luminosity galaxy may be able to survive digestion by a more massive galaxy with a more diffuse core, to create a "core within a core." Again in this case, one might expect merger remnants to have larger R_e/r_c ratios when compared to pristine galaxies of the same luminosity.

If in fact elliptical galaxies are not built up entirely by repeated cannibalization or hierarchical mergers, the issue still remains as to what extent any form of merging takes place at all. In the absence of a solid theoretical understanding of mergers, it is not possible *a priori* to identify any galaxies in the present sample as merger remnants, on the basis of their surface photometry profiles or subsequently measured parameters. On the other hand, it may well be that some of the scatter in the relationships between R_e and r_c or between L and ρ_c represents the effects of mergers on an otherwise unmodified population of elliptical galaxies formed in the initial epoch of galaxy formation. Whatever the case, the observed dependence of M/L on ρ_c and the Mg_2 index offers a further constraint on how merging galaxies intermix their stellar populations (or form new stars), in addition to the changes in physical scale discussed so far.

Externally, there is suggestive evidence that at least some objects in the present sample have in fact undergone mergers. Malin and Carter (1983) have found shells in the outer envelopes of NGC 1395 and NGC 4552, which Quinn (1982) suggests may have resulted from the recent merging of spiral galaxies with these systems. NGC 1395 has the second densest core of the class I galaxies, and NGC 4552 has one of the densest cores in the entire sample; any gas provided by the spirals may have increased the density of the preexisting cores by dissipative processes. The sample also contains a number of high-luminosity galaxies, such as NGC 741, NGC 1600, NGC

6086, and NGC 7768, which appear to be centrally located and dominant within their clusters. The latter two galaxies are cD's, which are commonly (although not universally) assumed to be the end products of mergers. These galaxies have the most *diffuse* cores of the present sample (although NGC 7768 is a class III galaxy and is likely to have a much denser core that is observed). NGC 1600, however, has one of the smallest R_e/r_c values (11.7) in the sample. It is not apparent how mergers could build up as luminous a galaxy as NGC 1600 without producing a much larger R_e/r_c ratio.

The common perception that first-ranked cluster galaxies have diffuse cores is often taken as evidence that these galaxies result from the homologous accretion of smaller galaxies, in light of the theoretical work of Hausman and Ostriker (1978). It is likely, however, that the cores of most cD galaxies are unresolved (Schweizer 1981*b*). Further, as noted above, *N*-body merger simulations do not verify the ad hoc assumption of homologous merging used by Hausman and Ostriker. Nevertheless, it is still interesting to consider the possibility of homologous mergers, since the brightest resolvable galaxies in this study generally do have diffuse cores. Homologous merging preserves the ratio of core to galaxy luminosity and the central velocity dispersion. This leads to a relationship between L, r_c, and I_0 of the form: $L \propto r_c^2 I_0$. Homology also predicts $L \propto R_e^2 I_e$. The former relationship appears to be inconsistent with the observed relationship between the core parameters given in equation (7), but is not far from it; in fact, the consistency of the sample with homologous mergers is much more suggestive in the observed relationship between luminosity and the effective radius parameters (see eq. [12]). Homologous mergers, however, cannot explain the observed scatter in ρ_c with respect to L and the even poorer relationship between ρ_e and L, which, if anything, would be expected to be a much stronger indicator of homologous mergers. In strictly homologous merging, luminosity density is strongly related to luminosity and does not act as an independent parameter. Homology also cannot produce the observed dependence of M/L on ρ_c and in fact would tend to smear out any such relationship if it existed in the progenitors. Last, the most serious difficulty of homologous mergers is that they preserve the central velocity dispersion, which is strongly at odds with the observed Faber-Jackson relationship.

VI. CONCLUSION

An important result from the present study is that many elliptical galaxies do have cores large enough to be resolved under good seeing conditions. The 14 class I galaxies have core radii larger than 1".5 and define a set of objects for which detailed structural analysis of the core is possible. The five class II galaxies (which have cores between 1".0 and 2".0) may be nearly resolved and may also provide useful glimpses into the central structure of elliptical galaxies, if observed under arcsecond seeing conditions. The class I and class II galaxies notwithstanding, however, this study also supports the conclusion of Schweizer (1979) that seeing effects are generally important and that, without any *a priori* knowledge of the intrinsic core structure, many elliptical galaxies must be considered to be unresolved. Slightly over half the galaxies in the sample fall into resolution class III, which means that these objects show little sign of resolvable cores at the 1" level of resolution. Since a typical seeing PSF causes more blurring than a final Wiener filter PSF of the same radius, in general sub-arcsecond seeing conditions will be required to resolve their cores. Although suitable seeing conditions might be found at some ground-based observatories, it is likely that the Space Telescope will be required to resolve the cores of class III galaxies. It appears difficult to predict *a priori* whether a given elliptical galaxy will be resolvable under given seeing conditions because of the independence of the core from the envelope; in general, however, it appears that seeing conditions such that $\Delta < R_e/90$ are required to ensure a 50% chance of core resolution.

The development of a hybrid Fourier deconvolution algorithm allows the observed luminosity profiles to be partially corrected for seeing in a model-independent way. Although a detailed analysis of the particular structure of the cores must await dynamical observations matching the present resolution, it is already clear that none of the 14 class I galaxies can be described by the isothermal cores of King models. Half of these galaxies strongly resemble the core luminosity profile of M87, and the remaining half have even more pronounced deviations from isothermality. This result may mean that massive nuclear black holes or radially anisotropic velocity fields, both of which have been proposed to be responsible for the morphology of the core of M87, occur generally in elliptical galaxies.

The present study finds that neither the core radius nor central surface brightness depends uniquely on total luminosity. Core radii correlate with luminosity but show significant scatter; central surface brightnesses show little dependence on luminosity. An analysis of total luminosity, central surface brightness, core radius, and central velocity dispersion shows these parameters to define a thin plane in their four-dimensional space which can be parameterized by total luminosity and central luminosity density. Although central luminosity density does correlate with the inverse cube of luminosity, it shows almost 2 orders of magnitude variation at some luminosity levels.

The measurement of core parameters allows central mass-to-light ratios to be calculated for a much larger set of galaxies than in any previous study. An examination of the effects of the present seeing-deconvolution algorithm verifies the results of previous numerical experiments that the central mass-to-light ratio is fairly insensitive to seeing effects. By parameterizing the mass-to-light ratio in terms of total luminosity and central luminosity density, it is seen that the mass-to-light ratio is independent of luminosity and depends on central luminosity density only. The central mass-to-light ratio is also found to correlate with the Mg_2 index, which verifies the results of other investigators using global mass-to-light ratios. Central luminosity density is found to be unrelated to the Mg_2 index, which means that the mass-to-light ratio is dependent on two separate parameters.

An analysis based on de Vaucouleurs effective radii and surface brightnesses produces results in parallel with the analysis of core properties; an average luminosity density derived from the surface photometry acts as a second parameter in addition to total luminosity to explain the observed scatter in the effective radius properties. Again, a global mass-to-light ratio appears to depend on the average luminosity density only, just as the central mass-to-light ratio depends only on the central luminosity density. The relationships between core and effective radius or central and average luminosity density, however, show considerable scatter and no dependence on any identifiable global property such as total luminosity.

The relationships between the core properties and those of the rest of the galaxy suggest that the cores were formed during

the final period of star formation in the protogalactic clouds that gave rise to elliptical galaxies. In this picture, the final density of the core depends strongly on the amount of gas left over from the initial period of star formation in the cloud and is thus sensitive to many different environmental effects during the epoch of galaxy formation which could add or remove gas from the galaxy. The properties of the core would then be fairly independent of global properties of the galaxy, as is observed. This picture might also explain the dependence of the mass-to-light ratio on luminosity density if the stellar mass function is influenced by the amount of dissipation allowed to take place in the core before star formation commenced. In contrast, although merging may account for some of the scatter in the observational parameters, the lack of any dependence of R_e/r_c on luminosity, the weakness of the dependence of central luminosity density on luminosity, and the dependence of the central mass-to-light ratio on central luminosity density appear difficult to explain if elliptical galaxies were formed by a hierarchy of mergers or by repeated cannibalization of small systems.

It is a pleasure to acknowledge the generous support, assistance, and counsel I received from my thesis adviser, Sandra M. Faber, throughout all phases of this work. Much of the analysis was beaten into shape through long conversations with Sandy. J. Jesus Gonzalez also provided much needed assistance with the analysis through his careful and patient tutorials on principal component analysis. I am also grateful to Richard J. Stover, who brought the CCD cameras at Lick Observatory into working order as scientific instruments, and who as coauthor of VISTA made crucial contributions to the software needed to carry out this work. This work was supported by NASA grant NSG 7503 and NSF grants AST 81-20960 and AST 82-115511.

REFERENCES

Allen, C. W. 1973, *Astrophysical Quantities* (London: Athlone), p. 162.
Bailey, M. E., and Sparks, W. B. 1983, *M.N.R.A.S.*, **204**, 53P.
Binney, J. 1982, *Ann. Rev. Astr. Ap.*, **20**, 399.
Binney, J., and Mamon, G. A., 1982, *M.N.R.A.S.*, **200**, 361.
Burstein, D., and Heiles, C. E. 1984, *Ap. J. Suppl.*, **54**, 33.
Davies, R. L., Efstathiou, G., Fall, S. M., Illingworth, G., and Schechter, P. L. 1983, *Ap. J.*, **266**, 41.
de Vaucouleurs, G. 1958, *Handbuch der Physik*, **53**, 275.
———. 1975, in *Stars and Stellar Systems*, Vol. **9**, *Galaxies and the Universe*, ed. A. Sandage, M. Sandage, and J. Kristian (Chicago: University of Chicago Press), p. 557.
de Vaucouleurs, G., de Vaucouleurs, A., and Corwin, H. R. 1976, *Second Reference Catalogue of Bright Galaxies* (Austin: University of Texas Press) (RC2).
Djorgovski, S. 1983, *J. Ap. Astr.*, **4**, 271.
Duncan, M. J., Farouki, R. T., and Shapiro, S. L. 1983, *Ap. J.*, **271**, 22.
Duncan, M. J., and Wheeler, J. C. 1980, *Ap. J. (Letters)*, **237**, L27.
Efstathiou, G., and Fall, S. M. 1983, preprint.
Faber, S. M. 1983, private communication.
Faber, S. M., and Jackson, R. E. 1976, *Ap. J.*, **204**, 668.
Farouki, R. T., Shapiro, S. L., and Duncan, M. J. 1983, *Ap. J.*, **265**, 597.
Geller, M. J., and Huchra, J. P. 1983, *Ap. J. Suppl.*, **52**, 61.
Hausman, M. A., and Ostriker, J. P. 1978, *Ap. J.*, **224**, 320.
Huchra, J. P., Davis, M., Latham, D., and Tonry, J. 1983, *Ap. J. Suppl.*, **52**, 89.
Huchra, J. P., and Geller, M. J., 1982, *Ap. J.*, **257**, 423.
Kendall, M. G. 1975, *Multivariate Analysis* (London: Griffin).
King, I. R. 1966, *A.J.*, **71**, 64.
King, I. R. 1978, *Ap. J.*, **222**, 1.
King, I. R., and Minkowski, R. 1972, in *IAU Symposium 44, External Galaxies and Quasi Stellar Objects*, ed. D. S. Evans (Dordrecht: Reidel), p. 87.
Kormendy, J. 1982, in *Morphology and Dynamics of Galaxies*, ed. L. Martinet and M. Mayor (Sauverny: Geneva Observatory), p. 113.
Kormendy, J. 1984, preprint.
Larson, R. B. 1974*a*, *M.N.R.A.S.*, **169**, 229.
———. 1974*b*, *M.N.R.A.S.*, **166**, 585.
———. 1975, *M.N.R.A.S.*, **173**, 671.
Lauer, T. R. 1985*a*, *Ap. J. Suppl.*, **57**, 473 (Paper I).
———. 1985*b*, *M.N.R.A.S.*, submitted.
Malin, D. F., and Carter, D. 1983, *Ap. J.*, **274**, 534.
Mould, J., Aaronson, M., and Huchra, J. 1980, *Ap. J.*, **238**, 458.
Nieto, J. L. 1983, *Astr. Ap. Suppl.*, **53**, 383.
Quinn, P. J. 1982, Ph.D. thesis, Mount Stromlo Observatory, Australian National University, Canberra.
Peterson, C. J., and King, I. R. 1975, *A.J.*, **80**, 427.
Sandage, A., and Tammann, G. A. 1981, *A Revised Shapley-Ames Catalog of Bright Galaxies* (Publication 635; Washington, D.C.: Carnegie Institution of Washington) (RSA).
Schechter, P. L. 1980, *A.J.*, **85**, 801.
Schweizer, F. 1979, *Ap. J.*, **233**, 23.
———. 1981*a*, *A.J.*, **86**, 662.
———. 1981*b*, *Ap. J.*, **246**, 722.
Terlevich, R., Davies, R. L., Faber, S. M., and Burstein, D. 1981, *M.N.R.A.S.*, **196**, 381.
Tinsley, B. M., and Larson, R. B. 1979, *M.N.R.A.S.*, **186**, 503.
Tonry, J. L., and Davis, M. 1981, *Ap. J.*, **246**, 666.
Villumsen, J. V. 1982, *M.N.R.A.S.*, **199**, 493.
White, S. D. M. 1982, in *Morphology and Dynamics of Galaxies*, ed. L. Martinet and M. Mayor (Sauverny: Geneva Observatory), p. 289.
Wiener, N. 1949, *Extrapolation, and Smoothing of Stationary Time Series* (New York: Wiley).
Young, P. J., Westphal, J. A., Kristian, J., Wilson, C. P., and Landauer, F. P. 1978, *Ap. J.*, **221**, 721.

TOD R. LAUER: Princeton University Observatory, Peyton Hall, Princeton, NJ 08544